

rhesie



This is to certify that the

thesis entitled

A Seismic Design Study of Two Deck-Type Arch Bridges

presented by

Dan Ping Xu

has been accepted towards fulfillment of the requirements for

Master of Science degree in Civil Engineering

R. C. Wew Major professor

Date November 9, 1992

O-7639

MSU is an Affirmative Action/Equal Opportunity Institution

LIBRARY Michigan State University

PLACE IN RETURN BOX to remove this checkout from your record. TO AVOID FINES return on or before date due.

DATE DUE	DATE DUE	DATE DUE
050		
		<u>-</u>

MSU Is An Affirmative Action/Equal Opportunity Institution ctcirclatedus.pm3-p.1

A SEISMIC DESIGN STUDY OF TWO DECK-TYPE ARCH BRIDGES

By

Dan Ping Xu

A THESIS

Submitted to
Michigan State University
in partial fulfillment of the requirements
for the degree of

MASTER OF SCIENCE

Department of Civil and Environmental Engineering

ABSTRACT

A SEISMIC DESIGN STUDY OF TWO DECK-TYPE ARCH BRIDGES

By

Dan Ping Xu

Two bridges were studied to provide information that could aid the designers of deck-type arch bridges, when considering seismic effects, regarding two parameters: 1) column diagonal bracing and 2) the depth to width ratio of the rib box section.

It was based on a computer modelling of the bridge and load system. Nonlinear elastic curved beam elements were used for the ribs, and straight beams and truss members for other members of the bridge. The seismic load was represented by the AASHTO design response spectrum.

It was noted that the column diagonal lateral bracing with small cross-sectional area when used at all panels is very effective in reducing the maximum stresses in the ribs.

It appears that the depth to width ratio of the rib section need not be increased for bridgs with longer spans if the cross-section area of the rib remains the same. This seems contrary to a general tendency in practice. The results indicate that the ratio need not go beyond two.

ACKNOWLEDGMENTS

The author wishes to express her deepest appreciation to Dr. Robert K. L. Wen of the Department of Civil and Environmental Engineering, Michigan State University, for his guidance in the preparation of this thesis and for his thought given throughout the course of this study. Thanks are also extended to the other members of the author's Master Degree Committee: Professors Frank Hatfield and Ron Harichandran for their guidance.

TABLE OF CONTENTS

LIST OF TABI	LES	vi
LIST OF FIGU	URES	vii
LIST OF SYM	BOLS	x
CHAPTER I	INTRODUCTION	1
CHAPTER II	MODELLING AND ANALYSIS METHOD	7
2.1 Gen	eral	7
2.2 Brid	ige Model	7
2.3 Dyn	namic Analysis	8
2.4 Gro	und Motion and Damping	9
2.5 Late	eral Tower Stiffness	9
2.6 Max	kimum Stresses	10
2.7 Max	kimum Response	11
2.8 Para	ameters	12
2.9 Con	nputer Modelling	13
CHAPTER III	DESIGN STUDIES	20
3.1 Gen	eral	20
3.2 Prel	iminary Parametric Studies	20
	3.2.1 Rotational restraint of supports	21

TABLE OF CONTENTS (continued)

3.2.2 Cross-sectional area of deck stringers A _s	21
3.2.3 Analysis method	22
3.2.4 Torsional constant	22
3.3 Natural Modes of Vibration for Out-of-plane Response	23
3.4 Comparison of Responses to Different Loadings	23
3.5 Effect of Cross-sectional Area of Column Diagonal	
Bracing A _d	24
3.6 Effect of Rib Depth to Width Ratio D/B	26
3.6.1 Sectional properties and natural frequencies	27
3.6.2 Effect on seismic responses	27
3.6.3 Effect on displacements and tower forces	29
3.6.4 Effect on responses to dead load and wind load	29
CHAPTER IV SUMMARY AND CONCLUSION	66
4.1 Summary	66
4.2 Concluding Remarks	68
LIST OF REFERENCES	69

LIST OF TABLES

Table 2-1.	Parameters of bridge system	
Table 2-2.	Parameters for in-plane and additional parameters	
	for out-of-plane studies	17
Table 3.2-1.	Effects of rotational restraint at supports on natural	
	frequencies (cps)	30
Table 3.2-2.	Effects of rotational restraint at supports on rib member	
	forces and stresses (MCSCB)	31
Table 3.2-3.	Effects of A _s on rib member forces and stresses	
	(MCSCB)	32
Table 3.2-4.	Effects of A _S on natural frequencies (cps)	33
Table 3.2-5.	Natural frequencies (cps) of MCSCB from different	
	analysis	34
Table 3.2-6.	Fundamental frequencies (cps) of MCSCB for different	
	AKTT values	35
Table 3.2-7.	Dynamic stresses (ksi) in MCSCB for different AKTT	
	values	35
Table 3.6-1.	Sectional properties of MCSCB for different D/B ratios	
	and t_f/t_w ratios	36
Table 3.6-2.	Sectional properties of MSSB for different D/B ratios	
	and t_f/t_w ratios	37
Table 3.6-3.	Displacements of MCSCB for different D/B ratios	38
Table 3.6-4.	Tower lateral forces (kips) of MCSCB for different	
	D/B ratios	38

LIST OF FIGURES

Figure 1-1.	A deck-type arch bridge	5
Figure 1-2.	Bridge model with global coordinates X, Y, Z and rib local	
	coordinates x, y, z, system is symmetric	6
Figure 2-1.	AASHTO acceleration spectra	18
Figure 2-2.	Box shape cross-section of arch rib	19
Figure 3-1.	First out-of-plain mode shape (2nd overall mode number)	39
Figure 3-2.	Second out-of-plain mode shape (4th overall mode number)	40
Figure 3-3.	Third out-of-plain mode shape (5th overall mode number)	41
Figure 3-4.	Fourth out-of-plain mode shape (7th overall mode number)	42
Figure 3-5.	Stress distributions under various loadings (MCSCB)	43
Figure 3-6.	Fundamental natural frequencies due to varying Ad	
	(MCSCB)	44
Figure 3-7.	Dynamic stresses due to varying Ad (Z-motion, MCSCB)	45
Figure 3-8.	Dynamic stresses due to varying Ad (Z-motion, MSSB)	46
Figure 3-9.	Fundamental natural frequencies of MCSCB due to	
	varying D/B ratio	47
Figure 3-10.	Stress and member forces at support due to varying	
	D/B ratio (MCSCB)	48
Figure 3-11.	Stress and member forces at the left node of panel 2 due	
	to varying D/B ratio (MCSCB), Z-motion seismic loading	49
Figure 3-12.	Stress and member forces at the left node of panel 3 due	
	to varying D/B ratio (MCSCB), Z-motion seismic loading	50

LIST OF FIGURES (continued)

Figure 3-13.	Stress and member forces at the left node of panel 4 due	
	to varying D/B ratio (MCSCB), Z-motion seismic loading	51
Figure 3-14.	Stress and member forces at the left node of panel 5 due	
	to varying D/B ratio (MCSCB), Z-motion seismic loading	52
Figure 3-15.	Dynamic stress distributions under lateral seismic loading	
	(Z-motion) due to varying D/B ratio (MCSCB)	53
Figure 3-16.	Dynamic stress distributions under in-plane seismic	
	loading (X-, Y-motion) due to varying D/B ratio (MCSCB)	54
Figure 3-17.	Dynamic stress distributions under three dimensional	
	loading (X-, Y-, Z-motion) due to varying D/B ratio (MCSCB)	55
Figure 3-18.	Dynamic stress distributions under lateral seismic loading	
	(Z-motion) due to varying D/B ratio (MSSB)	56
Figure 3-19.	Dynamic stress distributions under three dimensional	
	loading (X-, Y-, Z-motion) due to varying D/B ratio (MSSB)	57
Figure 3-20.	Stress and member forces at the left node of panel 2 due	
	to varying D/B ratio (MCSCB), dead load	58
Figure 3-21.	Stress and member forces at the left node of panel 3 due	
	to varying D/B ratio (MCSCB), dead load	59
Figure 3-22.	Stress and member forces at the left node of panel 4 due	
	to varying D/B ratio (MCSCB), dead load	60
Figure 3-23.	Stress and member forces at the left node of panel 5 due	
	to varying D/B ratio (MCSCB), dead load	61
Figure 3-24.	Stress and member forces at the left node of panel 2 due	
	to varying D/B ratio (MCSCB), wind load	62
Figure 3-25.	Stress and member forces at the left node of panel 3 due	
	to varying D/B ratio (MCSCB), wind load	63

LIST OF FIGURES (continued)

Figure 3-26.	Stress and member forces at the left node of panel 4 due	
	to varying D/B ratio (MCSCB), wind load	64
Figure 3-27.	Stress and member forces at the left node of panel 5 due	
	to varying D/B ratio (MCSCB), wind load	65

LIST OF SYMBOLS

A: acceleration coefficient

A_r: cross-sectional area of arch rib

 A_A : cross-sectional area of column bracing

 A_s : cross-sectional area of deck stringer

B: width of arch rib cross section

D: depth of arch rib cross section

E: Young's modulus

g: acceleration of gravity

G: dead load factor

H: rise or height of bridge arch

I_{xr}: moment of inertia of arch rib about local x-axis (resisting out-of-plane bending)

I ...: moment of inertia of arch rib about local y-axis (resisting in-plane bending)

[k]: stiffness matrix

K_t the torsional constants to be used for one rib

K_{tr}: the local torsional constant of one rib based on cross-section shape

k_{rih}: rib lateral stiffness

 k_{tow} : end tower lateral stiffness

L: length of the bridge span

M: Mass per foot of span length

 M_x : local bending moment about x-axis

 M_v : local bending moment about y-axis

N: number of panels

LIST OF SYMBOLS (continued)

[n1]: first order incremental stiffness matrices

[n2]: second order incremental stiffness matrices

Pz: member axial force

{q}: nodal displacement vector

r: radius of gyration of arch rib cross-section

S: site coefficient

S_x: section modulus about rib local x-axis (out-of-plane bending)

 S_{v} : section modulus about rib local y-axis (in-plane bending)

S_{A:} acceleration spectrum

S_m estimated maximum response (stress, member forces or displacements)

T: period of vibration

W: width of bridge

X, Y, Z:global coordinates

x, y, z rib local curvilinear coordinates

 ω_i ith circular frequency

 ξ : critical damping coefficient for first two modes

α: ratio of end tower lateral stiffness to rib system lateral stiffness

σ: total stress

CHAPTER I

INTRODUCTION

As lifeline structures, bridges in general should be sufficiently sound to continue functioning in an emergency situation such as that resulting from a major earthquake. Since the San Fernando earthquake in 1971, the engineering profession has given much added time and effort to the study of earthquakes in order to build stronger, safer structures. In the case of arch bridges, considerable amount of research had been done in recent years. In particular at MSU, several studies on the behavior of deck-type arch bridges (Fig. 1-1) had been made.

Research on the deck-type arch bridges was reported by Dusseau and Wen [3]. The importance of seismic effects on arch bridges was assessed. The seismic responses of three actual deck-type arch bridges: SSB (193ft); CSCB (700ft) and NRGB (1400ft) were computed and compared with those of wind (combined with dead load effects). It was concluded that seismic effects are important and can govern the design. However, the computations were based on linear straight beam elements to represent the arch rib. Artificial ground motions were applied.

C. M. Lee [6] developed a method of analysis and computer program that incorporated nonlinear curved beam elements for the arch rib. The geometric nonlinear analysis included was based on a model reported by Jose Lange [5]. The treatment of the elasto-plastic properties of the model was reported by Wen, Lee and Alahamd [15].

In applying Lee's analysis it was found when the duration of time of solution was sufficiently long, in the case of geometric nonlinearity, the equilibrium position would drift because of the use of the tangent stiffness matrix (the first incremental stiffness) in the solution to calculate the element resistance. In response to this challenge, a more

accurate secant stiffness matrix was developed for the nonlinear elastic curved beam element by Wen and Sunhedro [13]. With that the "drift" phenomenon would be removed.

The nonlinear element was subsequently incorporated by Wen [14] into a general program and used to obtain certain design aids for the in-plane response of deck type arch bridges. The design aids give response values in terms of stress and displacement amplification factors as functions of span length, L, and two major dimensionless parameters: the slenderness ratio, L/r, r is the radius of gyration of the rib cross-section, and the dead load factor $G = MgL^3/EI_{yr}$, where M is the total mass per unit length, E is the Young's modulus of elasticity, and I_{yr} is the moment of inertia of the rib section.

An exploratory study of three dimensional models concentrating on certain modelling aspects and the role of the end towers had been carried out by R. Millies [9]. Attention was turned to the development of information that could be helpful to the designers considering responses in the three dimensional space. In the latter case the number of variables of the problem was increased greatly over that for the two dimensional or in-plane case. It does not seem realistic to develop charts giving seismic responses covering all combinations of the numerous variables. However, it was recognized that not all variables are of equal significance. In his parametric variation study, by fixing the cross bracing truss elements between the ribs and the cross bars (straight beam elements) between the ribs, a study was made on the effects of the lateral stiffness of the end towers of the bridge system. Letting α be the ratio of the lateral stiffness of a tower to the lateral stiffness of the braced ribs, it was found that a value of α equal to two would be appropriate for seismic resistance. The study was based on time history solutions.

The preceding works all deal with the deck-type bridge. More recently A. Bellamine has completed a study of the seismic responses of tied-type of arch bridges [1]. It was limited to in-plane responses only. The practical effects of seismic loading in relation to design live load is assessed and an "optimal" distribution of material between the deck and the rib was investigated. Also it was found that, apart from the obvious fact that the deck would be subjected to additional axial stress on account of its function as a

tension tie, the seismic behavior of tied-type bridges seemed to be quite similar to that of deck-type bridges. A study of a single existing tied-bridge was also conducted by Lee and Torkamani [7]. It included considerations of soil structure interaction and unequal support motions.

The objective of this study is to get a better understanding of the general three dimensional seismic responses of deck type arch bridges. Thus the general purpose of the work reported herein is similar to that reported by B. Millies. Hence, the work may be considered as a continuation of same. That is: to develop information that may aid the designers in their decision making process.

The structural designer does not always get to decide on all the major parameters of the bridge, e.g., the span length and/or width of the bridge. However, the design of the cross-section of the arch rib generally falls within his/her domain. For most deck-type steel arch bridges, the rib cross-section usually has a box shape. A key parameter of that shape is the depth to width ratio. Its consideration is the main object of this study.

Another major parameter for the bridge design is the use, or lack of it, of diagonal bracing (perpendicular to traffic) between the columns supporting the deck (see Fig. 1-2). Although the qualitative action of these bracings is known, their effectiveness is not clear. Consequently such bracing had been used in some cases and omitted in others. A study of the effects of such bracings is the second objective of this report.

The study is based on the theory of elastic design. Hence, stress is regarded as the main response parameter. However, the nonlinear behavior of the ribs resulting from the dead load compression is considered. The seismic analysis is based on the design response spectrum approach.

Because of the large number of variables involved in the system considered, before data for investigating the previously mentioned two variables can be collected, it was necessary to conduct some preliminary studies leading to the holding of some parameters constant. They included the representation of the rotation restraint at the rib support, the cross-sectional area of the stringers of the deck and the representation of the torsional stiffness of the ribs.

In the following, Chapter 2 describes the modelling of the bridge system, the method of analysis, parameters of the bridge system and computer program used. The results obtained for the study are presented in Chapter 3. A summary and conclusion are given in Chapter 4.

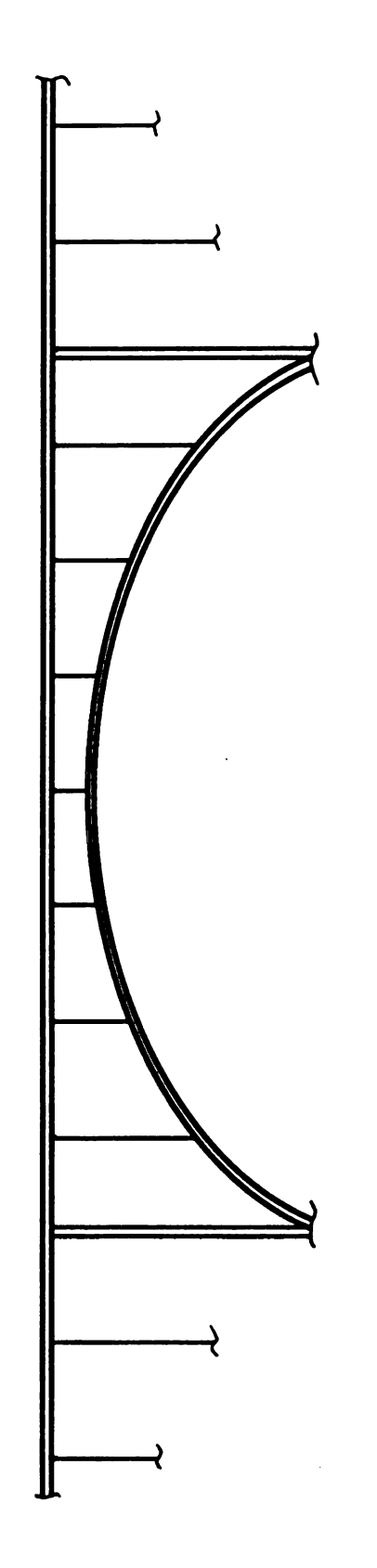
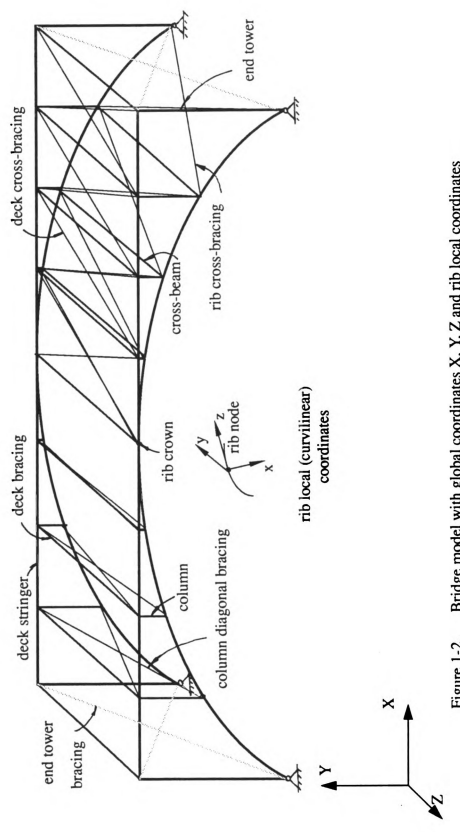


Figure 1-1. A deck-type arch bridge.



Bridge model with global coordinates X, Y, Z and rib local coordinates Figure 1-2.

x, y, z, system is symmetric.

CHAPTER II MODELLING AND ANALYSIS METHOD

2.1 General

This chapter discusses the modelling of the bridge system and the method of analysis. The parameters used, ground acceleration input, computer method of responses and the computer program are also described herein.

2.2 Bridge Model

In an arch bridge, the arch ribs are the main components of the structure. Therefore, the subsystem of the ribs is given greater precision than the other components such as the deck, column and the end towers.

The bridge model in the present study is a three dimensional finite element model (Fig.1-2). It contains two ribs (modelled by curved beams), which are parabolic in shape. The ribs are braced by cross-beam (modelled by straight beams) and cross-bracing (modelled by truss elements). Eight panels of equal length are used throughout the analysis.

The deck system, which includes the "deck stringers", "deck cross-bracing" and "deck bracings", is entirely represented by truss elements.

The deck and ribs are connected by "columns" modelled as truss elements which have larger stiffness. The cross-bracings between the columns at a given panel point are referred to as "column diagonal bracings."

The initial static load and the corresponding mass are assumed to be uniformly

distributed on the horizontal projection and lumped at the panel points.

2.3 Dynamic Analysis

The equation of motion of the bridge subjected to earthquake excitations may expressed as [6],

$$[m] \{\ddot{u}\} + [c] \{\dot{u}\} + \{r\} = -[m] \{\ddot{u}_{g}\}$$
 (1)

where, [m] is the lumped mass matrix,

- [c] is the damping matrix of the Rayleigh type,
- {r} is the resistance vector,
- {u} is the displacement vector with respect to the ground, and the dot superscripts denote derivatives with respect to time,
 - $\{\ddot{\mathbf{u}}_{\mathbf{g}}\}$ is the ground acceleration vector.

If linear elastic behavior is presumed,

$$\{r\} = [k] \{q\} \tag{2}$$

in which [k] is the element stiffness matrix and {q} is the displacement vector.

The resistance of a nonlinear elastic element may be written as

$$\{r\} = ([k] + \frac{[n1]}{2} + \frac{[n2]}{3}) \{q\}$$
 (3)

in which [n1] and [n2] are the first and second order incremental stiffness matrices [13].

2.4 Ground Motion and Damping

For dynamic analysis, the AASHTO [11] design response spectrum is used as the ground motion excitations for all three directions with the vertical acceleration scaled by a factor of 3/4. Using the multimode spectral method, the acceleration spectrum, S_A , is given by

$$S_{A} = \frac{1.2AS}{T_{m}^{2/3}} \tag{4}$$

for $T_m < 4.0$ second, and

$$S_{A} = \frac{3AS}{T_{m}^{4/3}} \tag{5}$$

for $T_m > 4.0$ second.

The value of S_A need not exceed 2.5A, as indicated in Fig. 2-1.

where A = acceleration coefficient, S = site soil coefficient and T_m = the period of the mth mode of vibration. The value of A = 0.4 and S = 1.0 correspond to the "strongest ground motion and soil" in the study.

Damping is assumed to be of the Rayleigh type with critical damping ratios of 0.02 used for the first two modes.

2.5 Lateral Tower Stiffness

The stiffness of the rib system, k_{rib} , is calculated using $F = k_{rib}$ z. A uniformly distributed load (F) in the z-direction is applied to the deck and ribs (with zero lateral end tower stiffness), and the corresponding crown displacement (z) is obtained. The stiffness is equal to the load applied divided by the displacement, i.e., $k_{rib} = F/z$. The

end tower lateral stiffness k_{tow} is set to be proportional to k_{rib} ,

$$k_{tow} = \alpha \times k_{rib}$$
 (6)

where α , is the ratio of the lateral stiffness of an end tower to that of the rib system. Following a suggestion in Millies' study [9], a value of two is used for α in this study.

Tower bracing area is then calculated as

$$A_{tb} = \frac{1}{2} \times \frac{k_{tow} \times l_{tb}^3}{EW^2}$$
 (7)

where E = Young's Modulus

W = width of the bridge

l_{th} = length of tow-bracing member

Once the tower bracing area A_{tb} is determined, the structure with the tower and tower bracings is then subjected to static load (dead load and wind load) and seismic load. Wind load is also applied to the structure in this study. The magnitude of wind load used corresponds to an horizontal acceleration of 0.1g of the bridge mass.

2.6 Maximum Stresses

The maximum stress at a given cross-section of a rib is calculated as

$$\sigma = \left| \frac{P_z}{A_r} \right| + \left| \frac{M_y}{S_v} \right| + \left| \frac{M_x}{S_x} \right| \tag{8}$$

where | | denotes the absolute value

 P_{τ} = axial force

 M_x , M_y = the local bending moment about the x-axis and the y axis, respectively

 S_{x} , S_{v} = the section moduli.

 $A_r =$ cross-sectional area of arch rib.

2.7 Maximum Response

For an estimated maximum dynamic response based on the response spectrum, the computer program used for the study can specify either by the complete quadratic combination method (CQC) or the square root of sum of squares (SRSS) method. In a preliminary study, no major difference was found among the results by using these two methods. Therefore CQC method, considered to be the more accurate of the two, was used throughout this study. That is,

$$S_{m} = \sqrt{\sum_{i} \sum_{j} S_{i} S_{j} P_{il} P_{jl} Q_{il} Q_{jl} R_{ij}}$$
(9)

$$R_{ij} = \frac{8 (C_i \omega_i + C_j \omega_j) \omega_i \omega_j \sqrt{C_i C_j \omega_i \omega_j}}{(\lambda \omega_i^2 - \lambda \omega_j^2)^2 + 4 C_i C_j \omega_i \omega_j (\omega_i^2 + \omega_j^2) + 4 (C_i^2 + C_j^2) \omega_i^2 \omega_j^2}$$
(10)

where

 S_{m} = estimated maximum response (stress, member forces or displacements)

 S_i = any modal response of the ith mode

1 = 1, 2, 3 corresponding to x,y,z ground motion, respectively

P_{i1} = participation factor

 ω_i = ith circular frequency

 Q_{il} = maximum response of SDOF system due to response spectrum

C_i = damping ratio of ith mode

The magnitude of p depends on the number of modes considered. It is observed in a preliminary study that the effect of those modes greater than 15 are negligible. Therefore, the number of modes used obtaining the results reported herein were set to be 20.

2.8 Parameters

The dimensional parameters that specify the bridge system being studied here are listed in the first two columns of Table 2-1. In a previous study [9], certain dimensionless parameters were defined from these basic dimensional ones and they were reproduced in Table 2-2. For the present study that deals with the cross-sectional design parameters, initially those dimensionless parameters such as I_{xr}/I_{yr} (ratio of moment of inertia about x-axis to that about y-axis for the rib), C_x/r_x (ratio of half width to the radius of gyration about x-axis of rib) and $G = MgL^3/EI_{yr}$ (the dead load displacement factor) were employed.

That approach was found to be unwieldy. Sometimes after translating them into dimensional form, impractical cross-sections resulted. For example, it was attempted to investigate the effect of G on the response of the bridge with different cross-sectional properties while keeping the cross-sectional area constant. When G is increased, in other words, I_{yr} must be decreased. Since all the other ratios are fixed at this point, hence I_{xr} has to be decreased. On the other hand if G is decreased, I_{xr} and I_{yr} are both in increasing. Meanwhile the cross sectional area A_r of the rib is fixed. One cannot expect such a cross-section.

Thus, assuming that the cross-sectional area has a box shape with two axes of symmetry (Fig. 2-2), the cross-sectional properties are defined by the depth D, width B, flange thickness t_f and web thickness t_w . For the study, the computer program computes first these from values from the data input cross-sectional area A_r , D/B ratio, t_w/D ratio, and t_f/t_w ratio. Since

$$A_{r} = 2t_{f}B + 2(D - 2t_{f})t_{w}$$
 (11)

the width B can be determined by

$$B = \sqrt{\frac{A_r}{2\left(\left(\frac{t_f}{t_w}\right)\left(\frac{t_w}{D}\right)\left(\frac{D}{B}\right) + \left(\frac{D}{B}\right)^2\left(\frac{t_w}{D}\right) - 2\left(\frac{t_f}{t_w}\right)\left(\frac{t_w}{D}\right)^2\left(\frac{D}{B}\right)^2\right)}}$$
(12)

Then D, $^t\mathbf{w}$, and $^t\mathbf{f}$ follow. The properties such that $I_{\mathbf{xr}}$ and $I_{\mathbf{yr}}$ can then be easily calculated.

2.9 Computer Modelling

The numerical results obtained for this study was obtained from a modified version of the program used in Millies [9]. The modifications include the following additions:

- (1). an analysis by use of response spectrum and model superposition.
- (2). an eigen analysis subroutine (Subroutine RSG)[4].
- (3). input and section properties computation associated with the rib box section (as described in the preceding section).

Table 2-1. Parameters of bridge system.

Parameter	er Description Values used		s used
	•	MCSCB	MSSB
L	length of the bridge span (ft.)	700.00	193.00
Н	rise of the bridge arch (ft.)	121.75	29.00
W	width of the bridge (ft.)	26.00	22.00
A _r	cross-sectional area of rib (ft ²)	2.59	0.96
I _{xr}	moment of inertia of rib about local x-axis (ft ⁴)	1.84 - 13.47	0.16 - 0.95
I _{yr}	moment of inertia of rib about local y-axis (ft ⁴)	20.91 - 34.90	1.37 - 2.13
Ktr	local torsional constant of one rib (see eq. 13)	6.51 - 21.46	0.61 - 1.61
C _{xr}	one half of the width of the rib cross-section (ft)	1.00 - 3.21	0.50 - 1.38
C _{yr}	one half of the depth of the rib cross-section (ft)	3.21 - 5.01	1.39 - 2.05
A _b	cross-sectional area of rib bracing beam (ft ²)	0.259	0.096
I _{xb}	moment of inertia of rib bracing beam about X-axis (ft ⁴)	1.45 - 1.75	0.60 - 1.07
I _{yb}	moment of inertia of rib bracing beam about Y-axis (ft ⁴)	1.45 - 1.75	0.60 - 1.07
Ktb	local torsional constant of bracing beam	1.45 - 1.75	0.60 - 1.07

Table 2-1. (continued)

r Description Values used		s used
	MCSCB	MSSB
cross-sectional area of stringer (ft ²)	0.40 - 2.00	0.80
cross-sectional area of column diagonal bracing (ft ²)	0.00 - 0.24	0.00 - 0.08
cross-sectional area of rib cross- bracing (ft ²)	0.00	0.00
cross-sectional area of deck bracing (ft ²)	4.00	4.00
cross-sectional area of deck cross-bracing (ft ²)	4.00	4.00
cross-sectional area of column (ft ²)	25.91	9.58
Young's modulus (ksf)	4176000	4176000
mass of the rib total mass (k/ft)	1.274	1.274
total mass per unit length of span length (k/ft)	4.80	4.80
ratio of end tower lateral stiffness to rib system lateral stiffness	2.00	2.00
critical damping coefficient for first two modes	0.02	0.02
number of panels	8	8
	cross-sectional area of stringer (ft²) cross-sectional area of column diagonal bracing (ft²) cross-sectional area of rib cross-bracing (ft²) cross-sectional area of deck bracing (ft²) cross-sectional area of deck cross-bracing (ft²) cross-sectional area of column (ft²) Young's modulus (ksf) mass of the rib total mass (k/ft) total mass per unit length of span length (k/ft) ratio of end tower lateral stiffness to rib system lateral stiffness critical damping coefficient for first two modes	cross-sectional area of stringer (ft²) cross-sectional area of column diagonal bracing (ft²) cross-sectional area of rib cross- bracing (ft²) cross-sectional area of deck bracing (ft²) cross-sectional area of deck cross-bracing (ft²) 4.00 cross-sectional area of deck cross-bracing (ft²) 4.00 cross-sectional area of column (ft²) Young's modulus (ksf) 4176000 mass of the rib total mass (k/ft) 1.274 total mass per unit length of span length (k/ft) 4.80 ratio of end tower lateral stiffness to rib system lateral stiffness to rib system lateral stiffness 2.00 critical damping coefficient for first two modes 0.02

Table 2-1. (continued)

Parameter	Description	Value MCSCB	s used MSSB
D	depth of arch rib cross section (in.)	76 - 120	33.4 - 49.2
В	width of arch rib cross section (in.)	24 - 77	12 - 33
t _f	flange thickness of arch rib cross section (in.)	1.7 - 2.8	1.48 - 2.2
t _w	web thickness of arch rib cross section (in.)	0.67 - 1.03	0.6 - 0.94
AKTT	torsional constant ratio (see section)	2 - 6	2

Table 2-2. Parameters for in-plane and additional parameters for out-of-plane studies [9]

Parameters for In-Plane Behavior	Range	Value Used
H/L	0.125 - 0.225	0.175
L/r,	100, 300	200
G	2.63 - 10.5	10.5
M,/M	0.344 - 0.760	0.265
N	6 - 24	8
ξ	2%, 5%	2%
c _y /r _y	1.00 - 1.55	1.27
L	200 - 1000 ft.	200, 600, 1000
X _g	0 - 0.50g	0.31g
Y _s	0 - 0.50g	0.23g
Additional Parameters for Out-of-Plane Behavior		
W	30 - 60	30
I_{xr}/I_{yr}	0.32 - 0.11	0.32 - 0.11
c _x /r _x	1.00 - 1.55	1.30
A _x /A _r	Not Available	0.04
A _b /A _r	0.10 - 0.25	0.10
I _{yb} /I _{yr}	0.0015 - 0.014	0.05
I_{xb}/I_{yb}	Not Available	1.0
K _{tb} /I _{yb}	Not Available	1.0
α	0.0 - 10.0	0 - 10
A,/A,	Not Available	0.183 - 0.91
z,	0 - 0.50g	0.31g

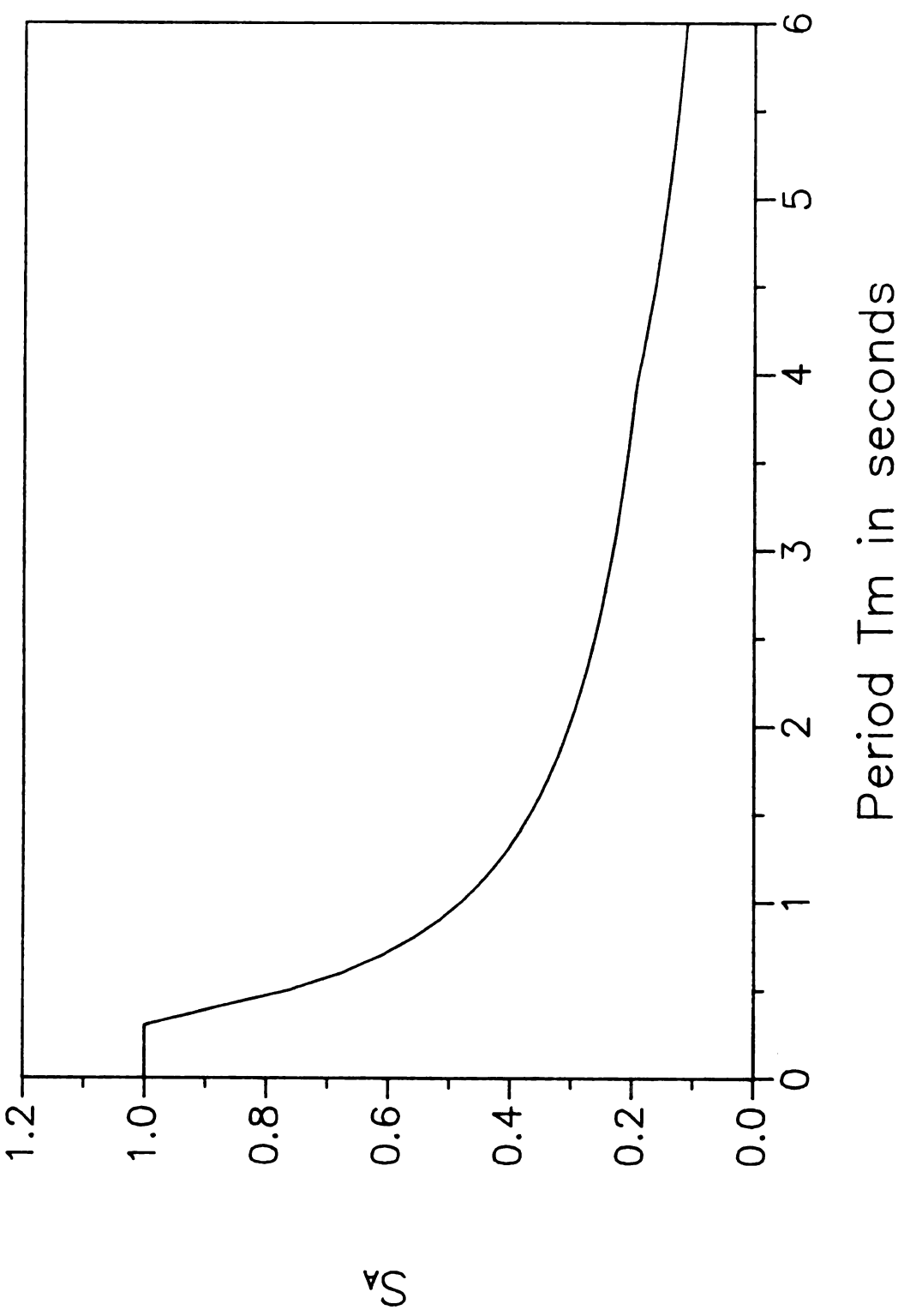


Figure 2-1. AASHTO acceleration spectra.

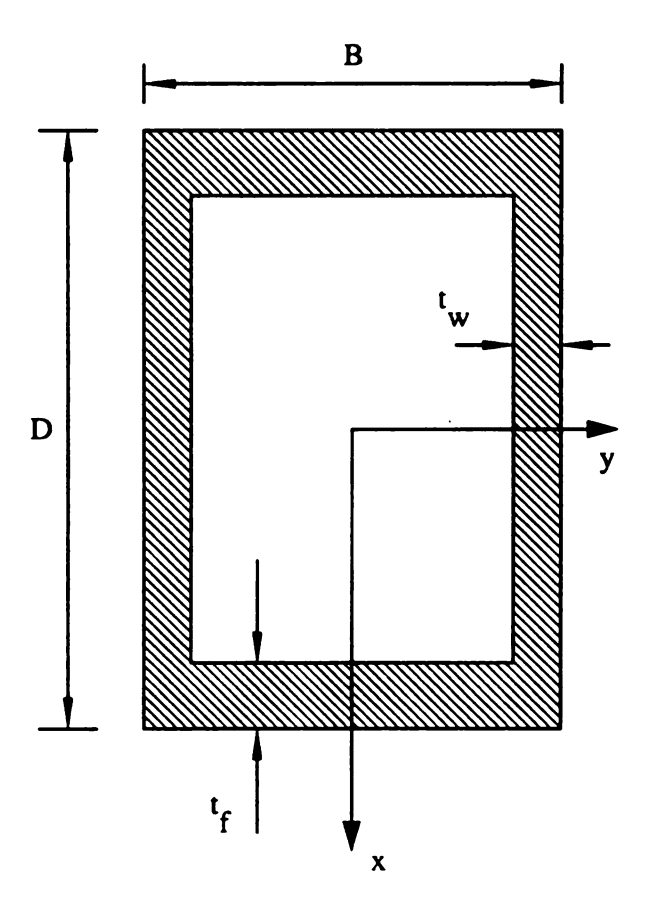


Fig. 2-2. Box shape cross-section of arch rib.

CHAPTER III DESIGN STUDIES

3.1 General

This Chapter presents and discusses the results obtained for the study. The study focuses on the MCSCB bridge, which is a medium span (700 ft.) and relatively slender bridge. Some results for MSSB, which is shorter (193 ft.) and less slender, are also presented. The values of other parameters of the two bridges are listed in Table 2-1.

Since much data is available on the in-plane response, the emphasis of the study is on the lateral response. Thus most data gathered corresponds to responses to ground motion in the lateral (Z) direction. For the purposes of comparison, dead load (DL) and static wind load (WL) responses are also presented as well as in-plane responses and the general case of responses to seismic excitations in all three directions in space.

Two major parameters are considered herein: A_d , the column diagonal bracing and D/B, the depth to width ratio of the rib section.

3.2 Preliminary Parametric Studies

Before numerical data on the effects of A_d and D/B were collected, a preliminary investigation was carried out to fixed certain parameters that enter into the analysis. This includes the type of restraint of supports, cross-sectional area of the deck stringers and the torsional constant used for the ribs.

3.2.1 Rotational restraint of supports

Previously in Millies' study [9], the out-of-plane rotations of the ribs at supports were restrained, i.e., rotation about the global X and Y axis are set to be zero at supports; the supports have moment release about the Z-axis only. In practice, it is possible that the bridge is not completely laterally fixed at supports, a model with free out-of-plane rotation at the rib supports was considered. The bridge investigated was MCSCB (with $A_d = 0$, $A_s = 0.4$ and AKTT = 2.0 to be defined later by using linear analysis method).

In Table 3.2-1 are listed the first five natural frequencies corresponding to the two cases of the rotational degrees of freedom about the global X - and Y-axis. It is seen that compared to fixed support model, the in-plane motion frequencies of the hinge support model remain the same, but the out-of-plane frequencies are decreased somewhat. This is due to the fact that releasing the moments about the X- and Y- axis does not change the in-plane behavior of the structure but reduces the out-of-plane stiffness of the structure.

In Table 3.2-2 are listed the stress resultants and stresses for the two cases. In general, releasing the restraint of out-of-plane rotation led to a reduction of the rib member forces and stresses at all nodes. As far as displacements are concerned, there was approximately a ten percent increase in the Z-direction due to the rotational releases.

Since bridge supports are not completely restraint in real cases, the "free" rotation model would provide more conservative results. Therefore, in the following studies, the supports are rotationally unrestrained.

3.2.2 Cross-sectional area of deck stringers A_s

Because of the deck support conditions, A_s has virtually no effect on the in-plane stiffness of the structure. Under out-of-plane loading, i.e., Z-load, however, the deck responds as a horizontal beam with the 2 edge stringers with cross-sectional area A_s acting as flanges. They do affect the lateral response.

In Table 3.2-3 are shown, for $A_s = 0.4$, 0.8 and 2.0 ft², the rib forces at the support, quart point and the crown for MCSCB (with $A_d = 0$, no rotational restraint at supports and AKTT = 2.0 (to be defined in the next section), MCSCB). It is seen that the internal forces of the rib decrease with increasing values of A_s (as the deck carries more load).

In Table 3.2-4 are listed for first five natural frequencies for the same bridge considered above. As expected, the frequencies corresponding to the in-plane modes (noted "I") are not affected by $A_{\rm S}$. The out-of-plane frequencies increase with an increase in $A_{\rm c}$.

For this study the intermediate value of A_s equal to 0.8 ft² was used.

3.2.3 Analysis method

The program has the capability of using a linear, geometrically nonlinear or "linearized" model for dynamic analysis. The "linearized" model employs the nonlinear model for the initial dead load solution, and the subsequent response to seismic motion would be calculated based on a linear analysis using the tangent stiffness of the structure under dead load as the linear stiffness.

The natural frequencies of MCSCB corresponding to the linearized and linear models are shown in Table 3.2-5 (with $A_s = 0.8$ ft², $A_d = 0.08$ ft², no rotational restraint at supports and AKTT = 2.0, MCSCB). It can be seen that the fundamental natural frequencies of the "linearized" structure are substantially lower than those of the linear model. The method of linearized analysis was chosen for use in this study.

3.2.4 Torsional constant

In an actual arch bridge construction, the two ribs are often braced together between the top flanges and the bottom ones. The two ribs and bracings would act as a single box section with a torsional stiffness substantially larger than the sum of the torsional stiffness of the individual rib sections. To account for this in the analysis model, the torsional parameter AKTT is introduced.

The parameter AKTT is the ratio of K_t to K_{tr} , where K_t is the torsional constants to be used for one rib, and K_{tr} is the torsional constant of the box section of one rib acting alone.

With an increase in AKTT, the structure becomes stiffer in out-of-plane response, while the in-plane stiffness would remain unchanged. In Table 3.2-6 (with $A_s = 0.8 \, \text{ft}^2$, $A_d = 0.08 \, \text{ft}^2$, no rotational restraint at supports, linearized analysis method, MCSCB), it is shown that AKTT does not affect the in-plane fundamental natural frequency but increase the out-of-plane fundamental frequency. However, the effect is quite small. Similarly, increasing the value of AKTT does not significantly influence the dynamic stresses as illustrated in Table 3.2-7. Therefore, AKTT equals 2.0 was used for the subsequent studies.

3.3 Natural Modes of Vibration for Out-of-plane Response

The vibration mode shapes of the first four modes for out-of-plane motion of the bridge are obtained for MCSCB and shown in Fig. 3-1, 3-2, 3-3 and 3-4. These four modes corresponding to 2nd, 4th, 5th and 7th overall mode number. For odd number out-of-plane motions (Fig. 3-1 and 3-3), the displacements of deck and ribs in the y direction are symmetric with respect to the crown plane of the bridge. Even number ones (Fig. 3-2 and 3-4) are anti-symmetric to the crown plane.

3.4 Comparison of Responses to Different Loadings

The maximum stresses in MCSCB at the various panel points under static vertical dead load, static lateral wind load, lateral seismic loading (Z-motion), two dimensional inplane seismic loading (X, Y motion) and three dimensional seismic loading (X, Y, Z motion) are plotted in Fig. 3-5. Due to the symmetry respect to the crown (Y-Z plane), results are presented for one half of the bridge. The dynamic response of the bridge by using the response spectrum method is symmetric. It is not so if time history analysis is used [9]

For combination of seismic loading, the amplification factors 1.0, 0.75, and 1.0 were applied to the ground acceleration in the X, Y and Z direction, respectively. For the different combinations of seismic loading, stresses were initially calculated under individual ground motion, then the total stresses were calculated based on those components as the square root of sum of squares.

As can be seen from the figure the stresses due to in-plane (X and Y direction) ground motion are the main components of the total stresses due to the three dimensional ground motion.

It is interesting to note that the seismic stresses from the lateral seismic loading have similar distribution as the stresses from the static wind loading. When the lateral seismic acceleration S_A is given by Equations (4) and (5), and the wind load corresponds to 0.1g, the values of the ratio of the seismic stress to the wind load stress at the various points are in the range of 2.4 to 2.9. This is also true for individual member forces. In other words, the behavior of the structure under wind load can be related to the one under seismic loading. If one likes to estimate the lateral seismic structure behavior, it is feasible to use a static lateral loading and apply a certain factor. The former seems much easier to deal with.

3.5 Effect of Cross-sectional Area of Column Diagonal Bracing A_d

In deck-arch bridge construction, column diagonal bracing has been used in some cases not in others. The role of the bracing is to help to tie the deck and the ribs together so as to act more as a unit in resisting lateral loads. Ultimately all lateral loads are carried to the foundation through the end towers and through the arch rib supports. The net effects of $^{A}_{d}$ on the structural response (i.e. stresses and displacements) are not clear. In this section, data on the responses with and without the bracings are presented.

Comparisons are made among the following cases:

- 1. no column bracing
- 2. column bracing at 1/4 points of the bridge with area of A_d equals to 0.38 percent of the rib area A_r
- 3. column bracing at each panel with A_d equals to 0.38 percent of A_r
- 4. column bracing at each panel with A_d equals to 1.5 percent of A_r
- 5. column bracing at each panel with A_d equals to 3 percent of A_r
- 6. column bracing at each panel with A_d equals to 9 percent of A_r .

Fundamental in-plane and out-of-plane frequencies of MCSCB due to various A_d values are illustrated in Fig. 3-6. As can be expected that, statically, the effect of the bracings is to increase the out-of-plane stiffness; and dynamically, the fundamental out-of-plane natural frequency is increased. The various cases with column diagonal bracings virtually have no effect on bridge in-plane frequencies. The behavior of the structure under in-plane loading is not affected by varying A_d .

Fig. 3-7 shows the maximum stress under lateral seismic load (Z-motion only) for MCSCB. It corresponds to those at the left end node of each curved beam member between the panel points of the rib. With column bracing, the stress at the crown decreased dramatically.

The values of A_d (ft²) used in the plot, presented as percentage of the rib area, are as follows,

	MCSCB	MSSB
0.38% A _r	0.01	0.0036
1.5% A _r	0.04	0.0144
3% A _r	0.08	0.0288
9% A _r	0.24	0.0864

Similar comparisons are plotted in Fig. 3-8 for MSSB. The stress responses have the same pattern as for the MCSCB except that stresses at the 1/8th points did not decreases as drastically.

It can be seen that the case of A_d equal to 0.38 percent rib area is most efficient in terms of decreasing rib member forces and stresses, especially at the crown node. In the case of no bracing, the maximum moment occurs at the crown. The column diagonal bracings reduce the moment at the crown by providing more points of lateral load transfer (in addition to the connection at the crown). The load redistribution is enhanced by increasing stiffness of column diagonal bracing.

The results obtained also indicated that column diagonal bracings can effectively reduce the dynamic stresses with relatively small members. It seems unnecessary and not economical to use too strong or heavy members. It is noticed that the effects of A_d leveled off after A_d reached approximately 3 percent of A_r . Therefore, an area of three percent of rib area A_r seemed desirable and was used in later studies. That is, $A_d = 0.08$ ft² for MCSCB; and $A_d = 0.03$ ft² for MSSB.

3.6 Effect of Rib Depth to Width Ratio D/B

The ribs of steel arch bridges often have cross-sections with a box shape (Fig. 2-2). Even assuming double symmetry, there are still a number of parameters that define the proportion of the cross-section. A key parameter is the depth to width ratio. The purpose of this section is to investigate its effect on the response of the bridge.

In Section 2.8, it was shown that the dimensions of a box section can be determined from the four parameters: the cross-section area A_r , the web thickness to depth ratio t_w/D , flange to web thickness ratio t_f/t_w and the depth to the width ratio D/B. Both the MCSCB and the MSSB were used in this study. For each bridge, A_r , t_w/D , t_f/t_w were held constant while D/B were varied from 1.0 to 5.0 for MCSCB, and 1.0 to 4.0 for MSSB respectively.

3.6.1 Sectional properties and natural frequencies

In order to aid the interpretation of the data to be presented, the various sectional properties of the cross-section, such as the section moduli, are presented in Table 3.6-1 for MCSCB and Table 3.6-2 for MSSB. In general, with an increase in the value of D/B (as the section narrows) there is large decrease in $I_{\chi r}$ (moment of inertia for out-of-plane bending) and a relatively modest increase in $I_{\chi r}$ (moment of inertia for in-plane bending).

The effects of D/B on the in-plane and out-of-plane natural frequencies of MCSCB are illustrated in Fig. 3-9.It is seen that with an increase in D/B ratio, there is a slight decrease in the out-of-plane frequency, although the increase in I_{xr} is large. The reason is thought to lie in the fact that the major source of the lateral stiffness of the bridge system still comes from the cross-sectional areas of the rib and the deck stringers and the "local" nature of I_{xr} has only a secondary effect. An increase in the D/B values resulted in increases in the in-plane frequency almost in proportion to the increase in I_{yr} which is the main source of the in-plane stiffness.

3.6.2 Effect on seismic responses

The effects of varying D/B on the stress resultants: P_z , M_x , M_y and the combined stress at the rib support due to lateral (Z) seismic motion are plotted in Fig. 3-10. There is very little effect of D/B on P_z at supports. The local moments M_x and M_y at supports are null. The total stress is caused by the axial force. P_z Thus, varying D/B ratio does not affect the stress σ at the support.

Member forces P_z , M_x , M_y and stress σ at the left end node of panel 2 are shown in Fig. 3-11. Again, P_z is not affected by D/B. At this node or the 1/8th point, M_y decreases about 26 percent when D/B increase from 1 to 3, and levels off approximately at D/B=3. The M_x distribution has a convex shape with the maximum occurring at D/B = 2.

Table 3.6-1 shows that an increase in D/B results in a drastic decrease in I_{xr} and significant decrease in the section modulus S_x while the changes in S_y are small. However, with an increase in D/B, the total dynamic stress did not increase as much as one might first think. This is because of the decrease in both M_x and M_y for D/B > 2.0, as illustrated in Fig. 3-11. The reader is reminded that these results were obtained with the cross-sectional area of the rib kept constant.

Dynamic rib member forces for the left end of members at the other panel points are shown in Fig. 3-12, 3-13 and 3-14 respectively. As previously, the total stress does not increase significantly. At the crown node, M_x decreases from 3245 ft.-k to 655 ft.-k, M_y increases from 474 to 1647 ft.-k, and P_z decrease from 548 kips to 395 kips. Consequently, the total dynamic stress decreases from 6.9 ksi to 5.1 ksi.

In Fig. 3-15 are shown the dynamic stresses due to the lateral ground motion as functions of the panel points with D/B as parameters. It is not surprising to note that the case D/B = 1 seems to yield the best "design". For D/B = 1, the stresses are generally lower except at the crown. But note that this stress is lower than that at panel point 2. The general nature of the results is expected because the load is in the lateral direction and a smaller D/B indicates a larger lateral stiffness.

In Fig. 3-16 are plotted, for in-plane seismic excitations (X and Y direction), similar data to those in Fig. 3-15. Here also the design D/B = 1.0 yields the lowest response (except at the support where the stresses are relatively small and the differences minor). This is not expected. The reasons may be (1) the in-plane section modulus S_y is not sensitive to D/B (Table 3.6-1) and (2) smaller D/B lowers the in-plane natural frequencies and also the acceleration response spectrum values (eq. (4) and (5)).

In Fig. 3-17 are shown similar plots to Fig. 3-16 for the case of seismic inputs in all three dimensions. Similar observations to those regarding Fig. 3-16 can be made.

In Fig. 3-18 and 3-19 are shown, for MSSB, the dynamic stresses due to lateral ground motion only and to all three dimensional ground motions, respectively. In these cases, the trends are less clear. However, larger values of D/B (3 or 4) are seen to be undesirable. The value of 1.65 (the actual value for SSB) seems the best.

3.6.3 Effect on displacements and tower forces

The effects of D/B on maximum displacements under lateral seismic motion are shown in Table 3.6-3. The largest vertical displacement scaled by the span length, Uy, occurred at the crown. It is seen that there is a moderate increase in Uy with an increase in D/B. It is believed that such an increase was due to the larger lateral torsional motion of the bridge resulting from a decrease in the lateral stiffness. The lateral displacement, scaled by span length, Uz, at the crown is an order of magnitude larger than Uy. As expected, it increased with increase in the D/B ratio.

The tower lateral force, F_z , represents the maximum horizontal reaction transferred at the support of an end tower. The effects of D/B on the tower lateral force are shown in Table 3.6-4. It is seen that they are relatively miner, of the order of one to two percent.

3.6.4 Effect on responses to dead load and wind load

The effects of D/B on the MCSCB rib internal forces due to dead load are illustrated in Figs. 3-20 to 3-23 for the various panel points. It is seen that, in general, such effects are quite small, even the in-plane bending moment, M_y , is seen to increase rather mildly with D/B. The total stress is practically independent of the D/B ratio.

The effects of D/B on the MCSCB rib internal forces due to (statically applied) wind load are illustrated in Figs 3-24 to 3-27. for the various panel points. The effects are seen to be more significant than those due to dead load. The considerable increase in out-of-plane bending, M_{χ} , as D/B increases from 1.0 to 2.0, is particularly noteworthy. For larger values of D/B, the increase in M_{χ} leveled off.

The out-of-plane bending, M_y , however, decreased, and the axial force P_z was not sensitive to the changes in D/B. The net effect on the maximum stress due to these stress resultants is a significant increase (of the order of 30%) from D/B = 1.0 to D/B = 2.0. For larger values of D/B the increase levelled off.

Table 3.2-1. Effects of rotational restraint at supports on natural frequencies (cps)

mode no.	fixed	free	
1	0.28913	0.27621	*0
2	0.31672	0.31672	Ι
3	0.64345	0.61210	0
4	0.77617	0.77617	I
5	0.88655	0.85064	0

* "O" denotes out-of-plane motion, and "I" denotes in-plane motion.

Table 3.2-2. Effects of rotational restraint at supports on rib member forces and stresses (MCSCB)

	fixed ¹⁾					free ²⁾		
×	My	Mz	٥	$P_{\mathbf{Z}}$	Mx	My	Mz	ď
(k-ft)	(k-ft)	(k-ft)	(k/ ft²)	(kips)	(k-ft)	(k-ft)	(k-ft)	(k/ ft²)
4142	0	1930	2642	2470	0	0	0	953.0
1972	484.7	2887	849.6	193.5	1865	432.9	3439	840.8
2822	1838	1395	1745	1168	2702	1741	1561	1749

1). rotations at supports about X and Y axies are restrained.
2). rotations at supports about X and Y axies are not restrained.

Table 3.2-3. Effects of A_s on rib member forces and stresses (MCSCB)

		A A	$A_{S} = 0.4 \text{ ft}^{2}$			A S	$A_{S} = 0.8 \text{ ft}^{2}$			*S	$A_{S} = 2.0 \text{ ft}^{2}$	
	Pz	×	M	ь	Pz	×	M _y	ь	Pz	×	M	ь
	(kips)	(k-ft)	(k-ft)	(k/ ft²)	(kips)	(kips) (k-ft)	(k-ft) (k/ft²)	(k/ ft²)	(kips)	(kips) (k-ft)	(k-ft) (k/ft ²)	(k/ ft²)
support, member 1 left end	2470	0	0	953.0	2237	0	0	863.4	1874	0	0	723.1
1/4 point, member 3 left end	193.5	1865	432.9	840.8	178.0	1669	416.9 757.3	757.3	162.1	1366	390.1	627.2
crownt, member 5 left end	1168	2702	1741	1749	1037	2357	1556	927.6	839.5	1819	1306	1213

Table 3.2-4. Effects of A_S on natural frequencies (cps)

mode no.	$A_{S} = 0.4 \text{ ft}^{2}$	$A_{S} = 0.8 \text{ ft}^{2}$	$A_{S} = 2.0 \text{ ft}^{2}$
1	0.27621 (O)*	0.29961 (O)	0.31673 (I)
2	0.31673 (I)	0.31673 (I)	0.34021 (O)
3	0.61210 (O)	0.66287 (O)	(O) 8E0020
4	(I) 71977.0	0.77617 (I)	(I) L1971-0
\$	0.85064 (O)	0.92843 (O)	1.05426 (O)

* "O" denotes out-of-plane motion, and "I" denotes in-plane motion.

Table 3.2-5. Natural frequences (cps) of MCSCB from different analysis

Mode No.	Linearized	Linear	
1	0.27101	0.31673	I*
2	0.31028	0.32247	0
3	0.72896	0.77617	I
4	0.78125	0.79034	О
5	1.25722	1.26190	О
6	1.39736	1.44537	I
7	1.80682	1.81774	О
8	1.82029	1.85972	О
9	1.89594	1.93431	О
10	2.05909	2.09128	I
11	2.43652	2.45350	I
12	2.45858	2.49048	О
13	2.65667	2.66017	0
14	3.01787	3.05821	I
15	3.03041	3.08334	0
16	3.43868	3.50449	О
17	3.86869	3.90187	0
18	3.90001	3.93363	I
19	4.23250	4.23362	I
20	4.34983	4.37691	Ο

^{* &}quot;I": denotes in-plane (X-Y plane) and "O": denotes out-of-plane (Y-Z plane).

Table 3.2-6. Fundamental Frequencies (cps) of MCSCB for different AKTT values

	AKTT=2	AKTT=3	AKTT=4	AKTT=6
in-plane	0.27101	0.27101	0.27101	0.27101
out-of-plane	0.31028	0.31143	0.31223	0.31325

Table 3.2-7. Dynamic stresses (ksi) in MCSCB for different AKTT values

	AKTT=2	AKTT=3	AKTT=4	AKTT=6
support	7.653	7.576	7.521	7.458
1/8 points	10.688	10.868	11.014	11.215
1/4 points	4.367	4.430	4.490	4.548
3/8 points	3.416	3.375	3.367	3.349
crown	5.465	5.233	5.111	5.174

Sectional properties of MCSCB for diferent D/B ratios and \(\text{t} / \text{t}_w \) ratios Table 3.6-1.

						 												_							
Kt	21.460	15.567	11.251	8.417	805.9	49.194	29.323	18.611	12.727	9.217	29.323	20.027	13.830	10.007	7.545	18 611	13.830	10.193	7.740	6.053	12.727	10.007	7.740	6.104	4.920
Sy	6.5125	7.1470	7.1986	7.1016	6.9670	7.3651	7.0811	6.7507	6.4995	6.3113	6.9162	7.2703	7.1640	6.9842	6.8073	53163	7.0552	7.1771	7.1222	7.0124	5.7790	6.7295	7.0235	7.0855	7.0524
Sx	4.1960	3.1243	2.5338	2.1319	1.8349	7.3651	4.8905	3.6469	2.8895	2.3789	5.0071	3.6352	2.8803	2.3793	2.0186	3 8075	2.9247	2.3924	2.0275	1.7556	3.2498	2.4693	2.0560	1.7714	1.5557
lyr	20.9078	28.8687	32.3948	34.0791	34.9001	31.9521	35.5240	35.9473	35.7606	35.4515	24.5344	31.6798	34.2568	35.2450	35.5880	19 4194	27.5456	31.4126	33.3885	34.4298	15.8981	24.0133	28.5147	31.1507	32.7479
ואנ	13.4710	6.3101	3.8009	2.5576	1.8384	31.9521	12.2672	6.4731	3.9745	2.6725	17.7620	7.9200	4.5909	3.0017	2.1107	11 9824	5.7095	3.4903	2.3762	1.7239	8.9402	4.4056	2.7824	1.9469	1.4448
.*	0.0557	0.0701	0.0781	0.0833	0.0870	0.0753	0.0871	0.0924	0.0955	0.0975	0.0616	0.0756	0.0830	0.0876	0.0908	0.0534	0.0678	0.0760	0.0814	0.0852	0.0478	0.0619	0.0705	0.0763	90800
J	0.1486	0.1870	0.2083	0.2222	0.2319	0.0753	0.0871	0.0924	0.0955	0.0975	0.1232	0.1513	0.1660	0.1752	0.1815	0.1601	0.2033	0.2279	0.2441	0.2557	0.1910	0.2478	0.2819	0.3053	0.3224
D	6.4209	8.0786	9.0003	9.5976	10.0187	8.6766	10.0335	10.6499	11.0041	11.2343	7.0948	8.7148	9.5635	10.0928	10.4559	6.1488	7.8086	8.7536	9.3759	9.8197	5.5020	7.1367	8.1198	8.7928	9.2870
В	6.4209	4.0393	3.0001	2.3994	2.0037	8.6766	5.0168	3.5500	2.7510	2.2469	7.0948	4.3574	3.1878	2.5232	2.0912	6.1488	3.9043	2.9179	2.3440	1.9639	5.5020	3.5683	2.7066	2.1982	1.8574
A _r	2.5911	2.5911	2.5911	2.5911	2.5911	2.5911	2.5911	2.5911	2.5911	2.5911	2.5911	2.5911	2.5911	2.5911	2.5911	2.5911	2.5911	2.5911	2.5911	2.5911	2.5911	2.5911	2.5911	2.5911	2.5911
t _w /D	0.00868	0.00868	0.00868	0.00868	0.00868	0.00868	0.00868	89800.0	89800.0	0.00868	0.00868	0.00868	0.00868	0.00868	0.00868	0.00868	0.00868	0.00868	0.00868	0.00868	0.00868	0.00868	0.00868	0.00868	0.00868
رد/ر _w	2.67	2.67	2.67	2.67	2.67	-	_	-	_	-	2	2	2	2	7	65	. 6	3	3	3	4	4	4	4	4
D/B	1	7	6	4	s	-	7		4	2	_	2	3	4	2		2	3	4	2	-	2	3	4	5

Sectional properties of MSSB for diferent D/B ratios and '1/1, ratios Table 3.6-2.

Кu	1.608	1.153	0.824	0.611	3.141	1.886	1.201	0.823	1.886	1.307	0.910	0.663	1 201	0.910	0.680	0.521	600	0.823	0.663	0.521	0.417	
Sy	0.9823	1.0596	1.0561	1.0347	1.1030	1.0594	1.0084	0.9695	1.0182	1.0724	1.0562	1.0284	0.9122	1.0237	1.0430	1.0349	00.00	0.81/8	0.9590	1.0044	1.0148	
S _x	0.6816	0.4953	0.3913	0.3209	1.1030	0.7200	0.5267	0.4089	0.7491	0.5362	0.4179	0.3391	0.5822	0.4312	0.3477	0.2899	17070	0.4847	0.3636	0.2987	0.2537	
lyr	1.3697	1.8463	2.0411	2.1257	1.9779	2.2007	2.2255	2.2119	1.4956	1.9419	2.1035	2.1645	1 1623	1.6646	1.9075	2.0322		0.9329	1.4273	1.7081	1.8749	
Ixr	0.9504	0.4315	0.2521	0.1648	1.9779	0.7478	0.3874	0.2332	1.1004	0.4855	0.2774	0.1784	0.7418	0.3506	0.2119	0.1423	06330	0.5550	0.2706	0.1694	0.1172	
>	0.0530	0.0662	0.0734	0.0780	0.0681	0.0789	0.0838	0.0866	0.0558	0.0688	0.0756	0.0799	0 0484	0.0617	0.0695	0.0746	0 0423	0.0433	0.0565	0.0646	0.0702	
u u	0.1236	0.1544	0.1712	0.1820	0.0681	0.0789	0.0838	0.0866	0.1116	0.1375	0.1513	0.1599	0 1452	0.1852	0.2084	0.2237	20170	0.1733	0.2261	0.2583	0.2807	
Q	2.7888	3.4848	3.8652	4.1089	3.5864	4.1546	4.4138	4.5631	2.9378	3.6216	3.9830	4.2097	2 5483	3.2521	3.6579	3.9274	3100.0	C197:7	2.9767	3.4013	3.6953	
æ	2.7888	1.7424	1.2884	1.0272	3.5864	2.0773	1.4713	1.1408	2.9378	1.8108	1.3277	1.0524	2 5483	1.6261	1.2193	0.9819	31000	C197.7	1.4883	1.1338	0.9238	
۲.	0.9583	0.9583	0.9583	0.9583	0.9583	0.9583	0.9583	0.9583	0.9583	0.9583	0.9583	0.9583	0.9583	0.9583	0.9583	0.9583	0.0502	0.9383	0.9583	0.9583	0.9583	
t _w /D	0.01899	0.01899	0.01899	0.01899	0.01899	0.01899	0.01899	0.01899	0.01899	0.01899	0.01899	0.01899	0.01899	0.01899	0.01899	0.01899	000	0.01899	0.01899	0.01899	0.01899	
رد/ _د س	2.33	2.33	2.33	2.33	_	_	_	-	2	7	2	2	~,	, w	3	3	•	4	4	4	4	
D/B	1	7	6	4	_	2	3	4	_	2	3	4	-	. 6	6	4	•	-	7	3	4	

Table 3.6-3. Displacements of MCSCB for different D/B ratios

	U	z (×10 ⁻²	²)		Uy(×1	0 ⁻⁴)
D/B	tower to	p 1/4pt	crown	1/8 pt	1/4 pt.	crown
1 2 3	0.0412	0.224	0.329	0.323	0.831	2.06
	0.0411	0.225	0.331	0.298	0.792	2.10
	0.0414	0.229	0.335	0.297	0.764	2.21
4	0.0417	0.232	0.340	0.306	0.741	2.32
5	0.0420	0.235	0.344	0.318	0.722	2.42

Table 3.6-4. Tower lateral force (kips) of MCSCB for different D/B ratios

D/B	Fz
1	308.78
2	308.82
3	307.26
4	305.52
5	303.93

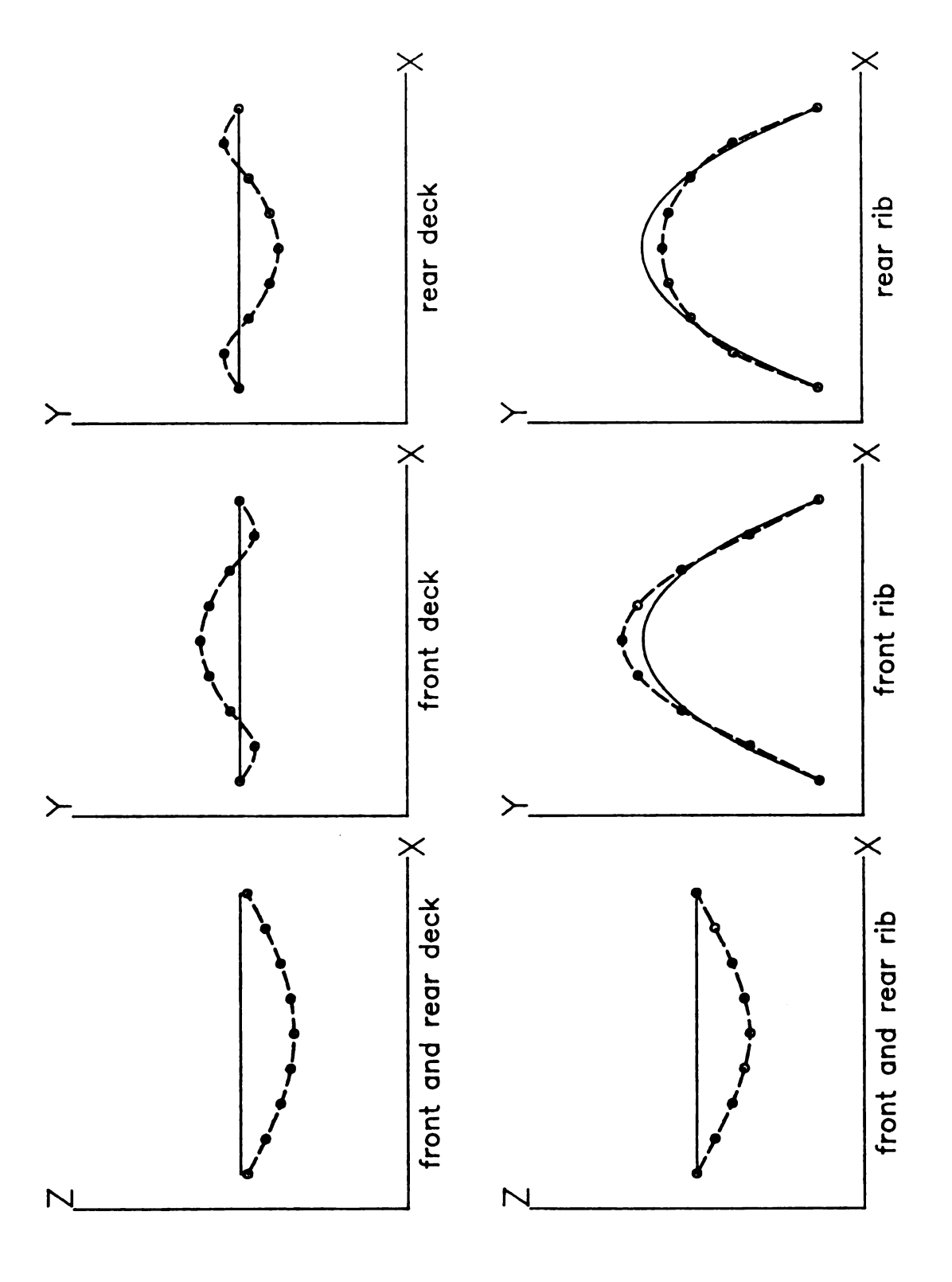


Figure 3-1. First out-of-plain mode shape (2nd overall mode number).

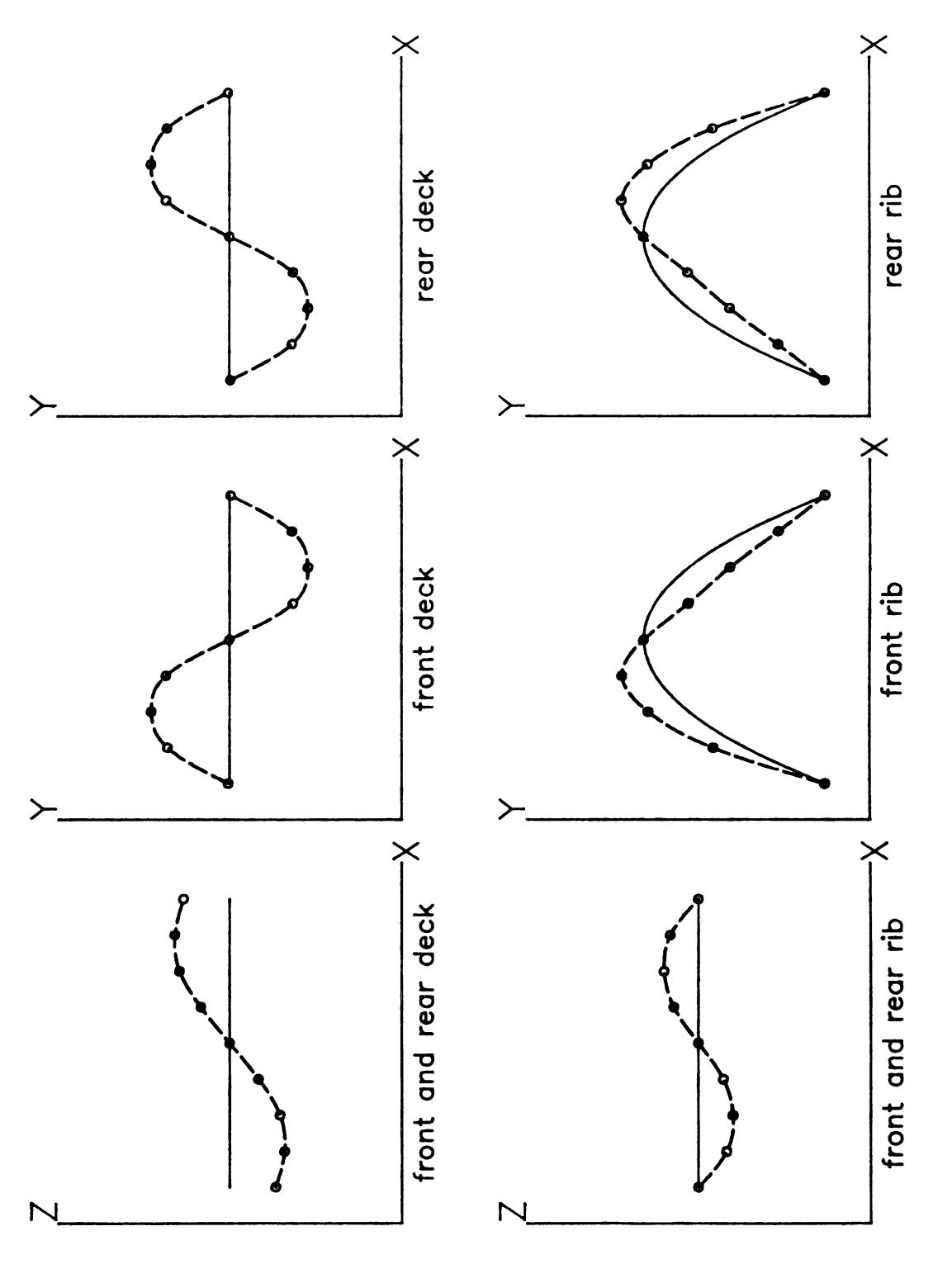


Figure 3-2. Second out-of-plain mode shape (4th overall mode number).

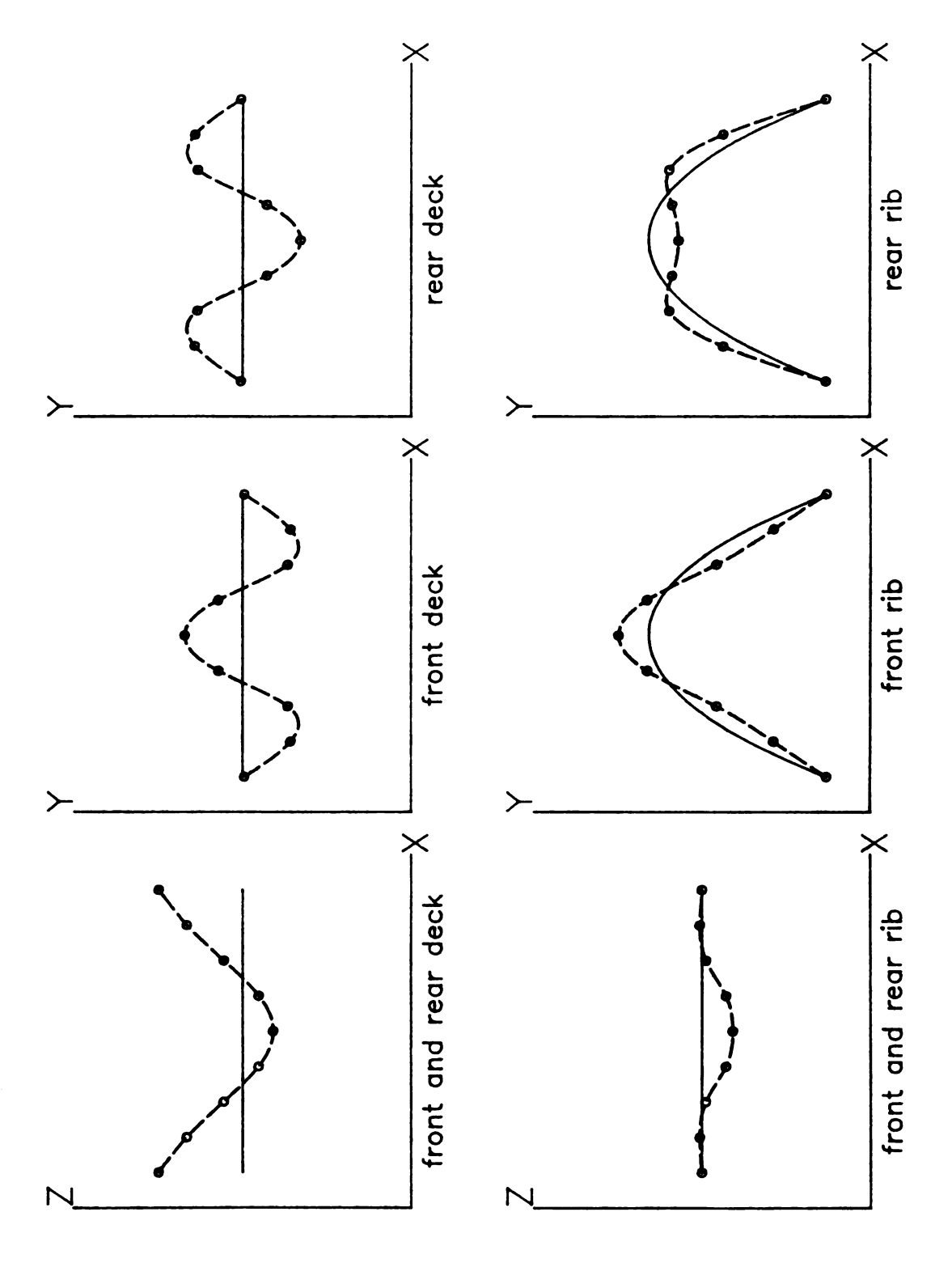


Figure 3-3. Third out-of-plain mode shape (5th overall mode number).

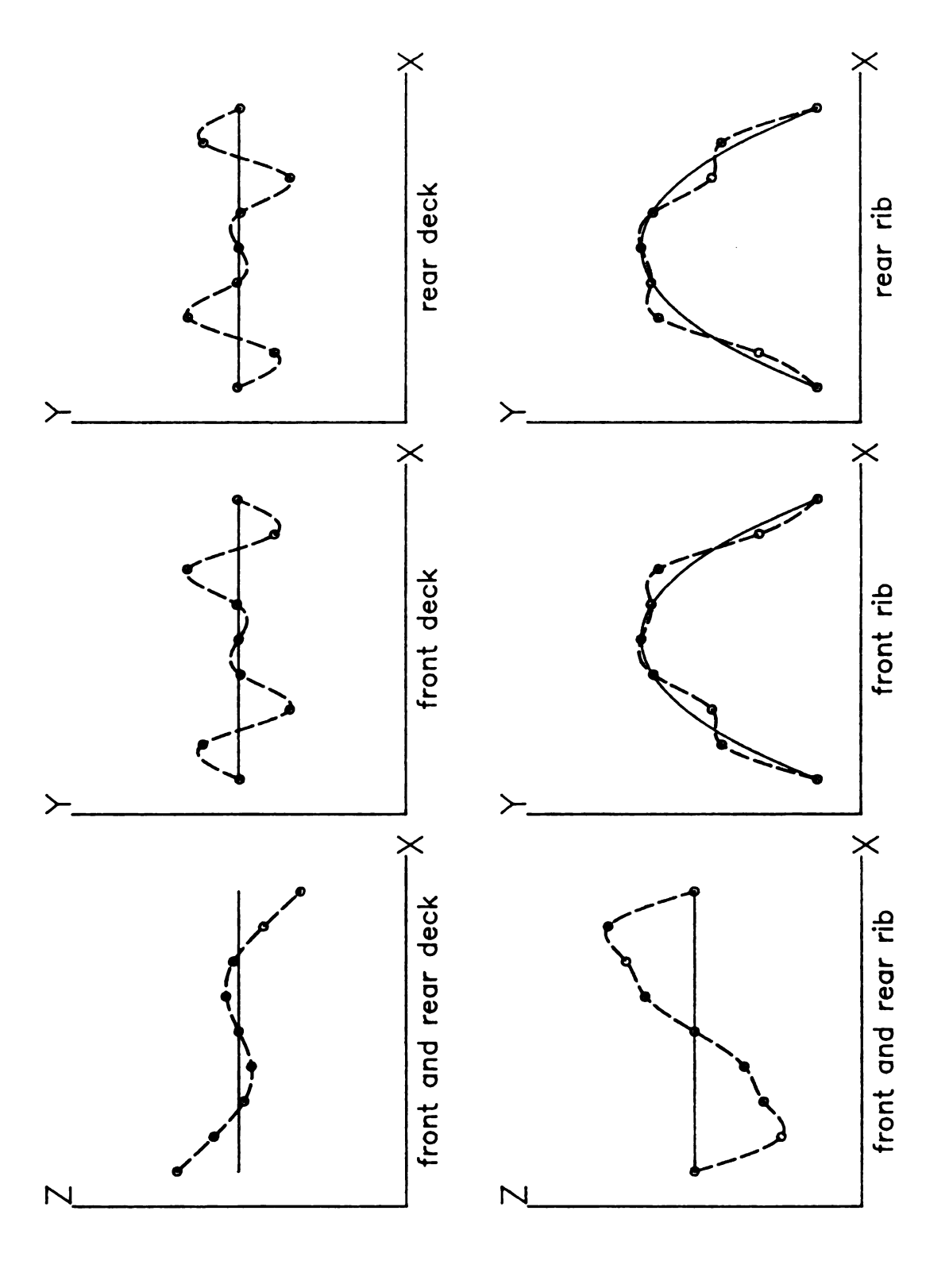
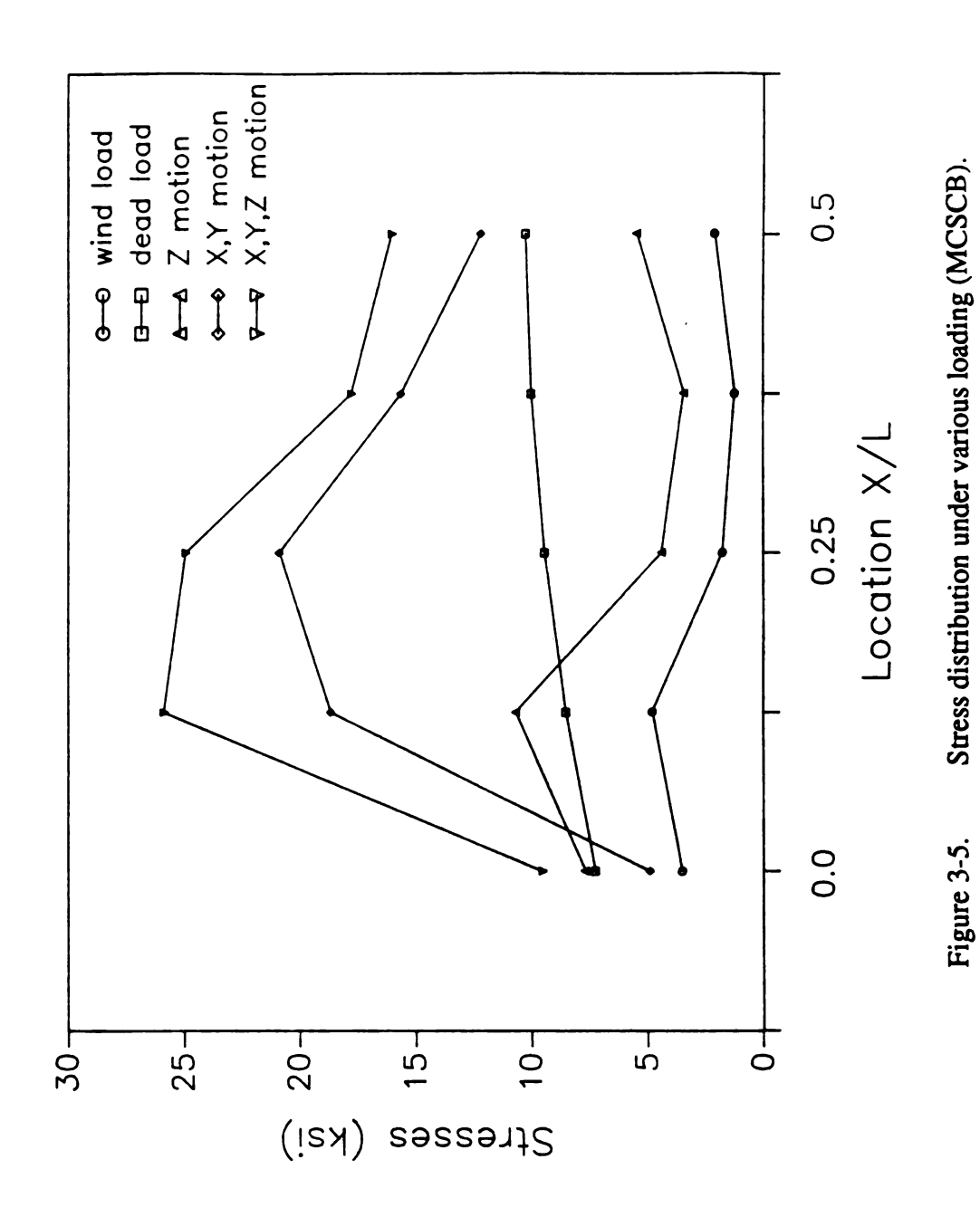
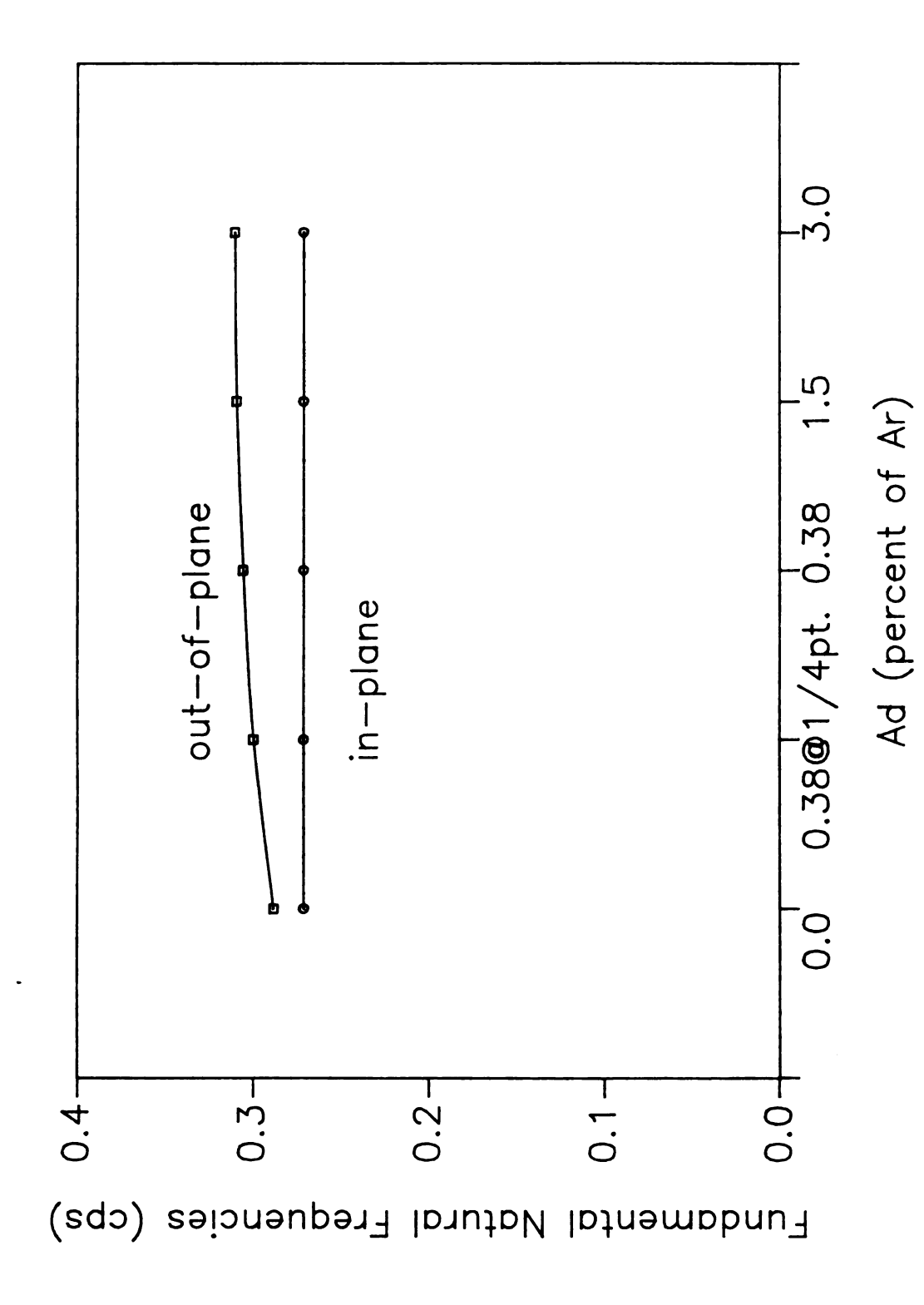


Figure 3-4. Fourth out-of-plain mode shape (7th overall mode number).





Fundamental natural frequencies due to varying Ad (MCSCB). Figure 3-6.

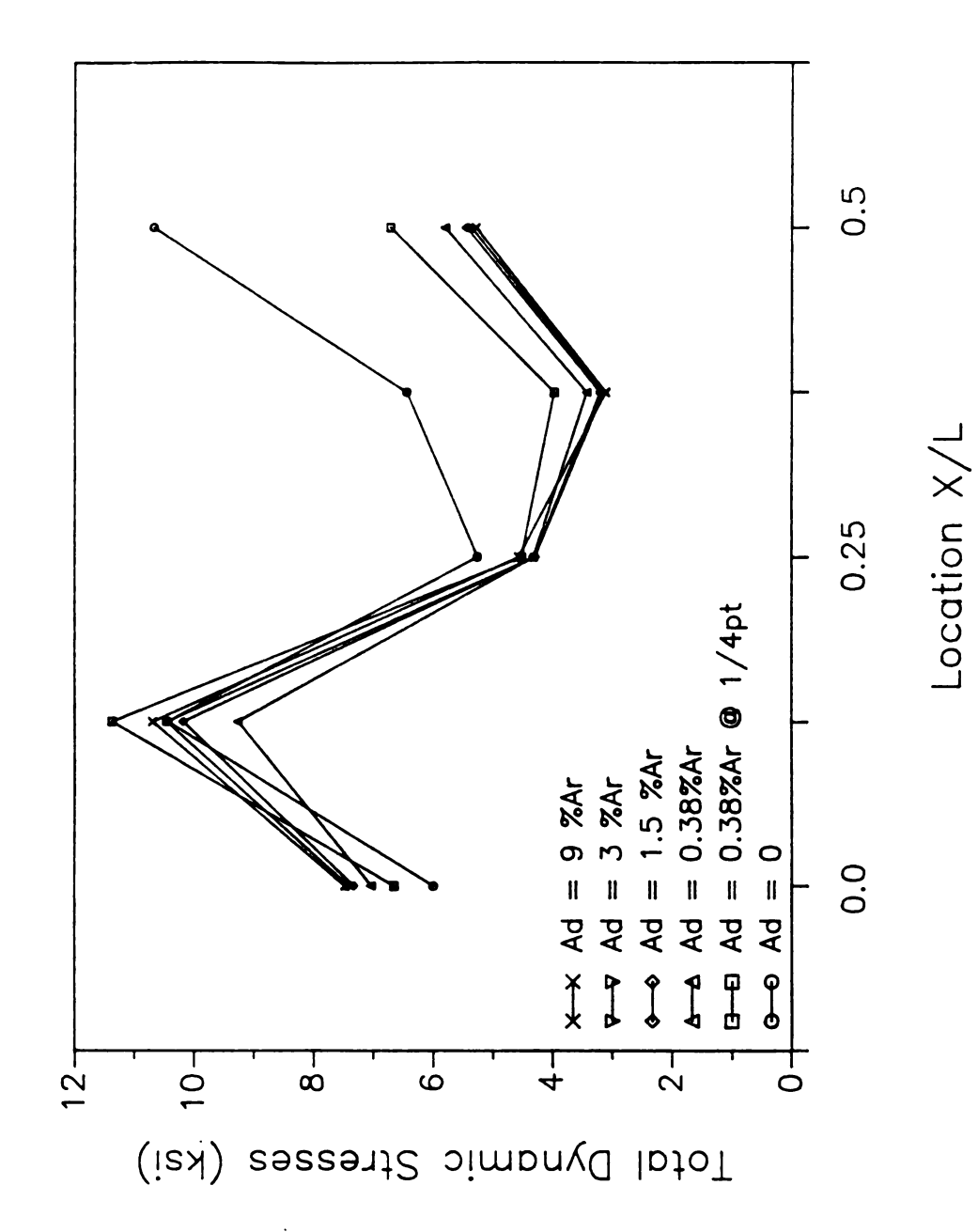


Figure 3-7. Dynamic stresses due to varying Ad (Z-motion, MCSCB).

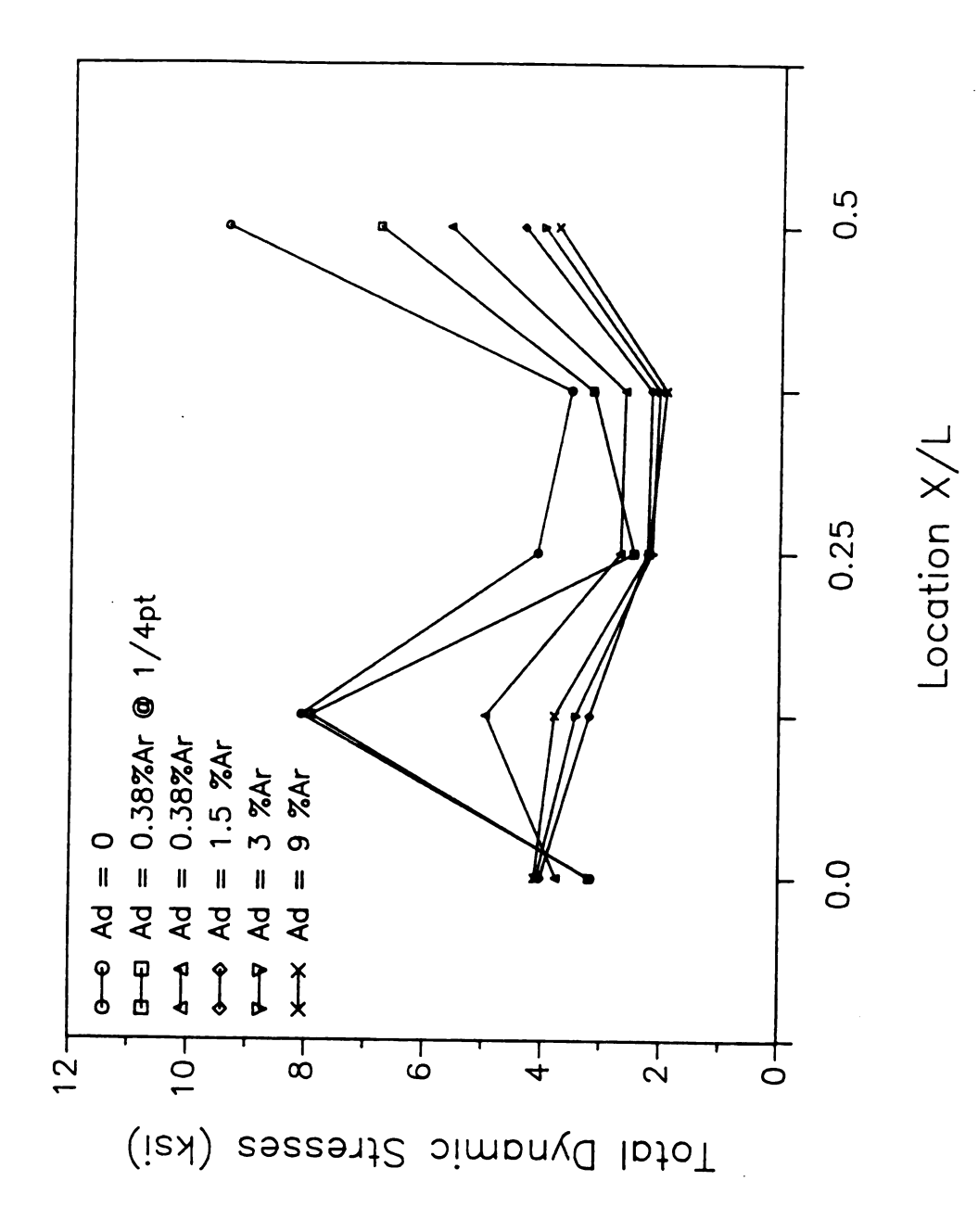
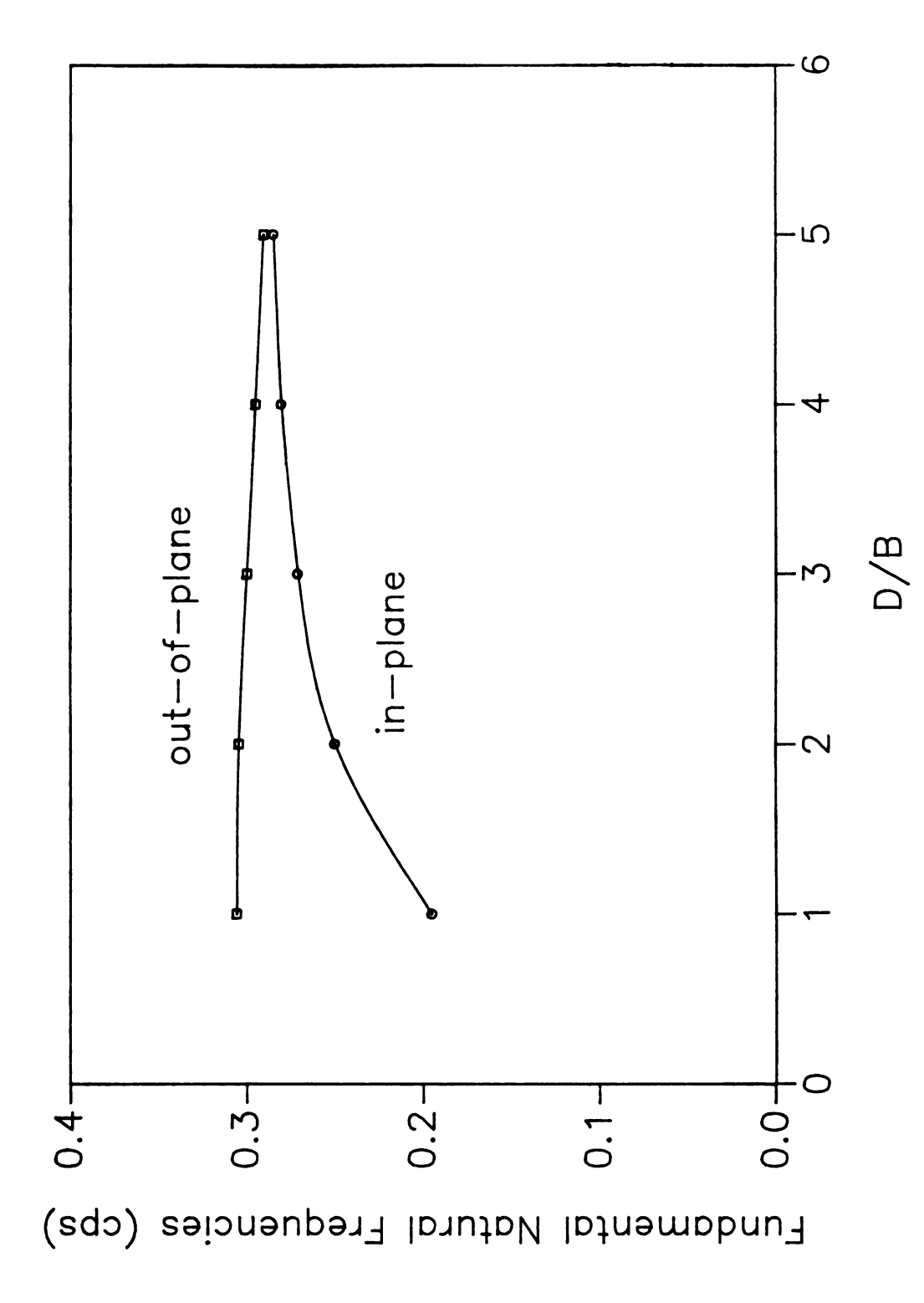


Figure 3-8. Dynamic stresses due to varying Ad (Z-motion, MSSB).



Fundamental natural frequencies of MCSCB due to varying D/B ratio. Figure 3-9.

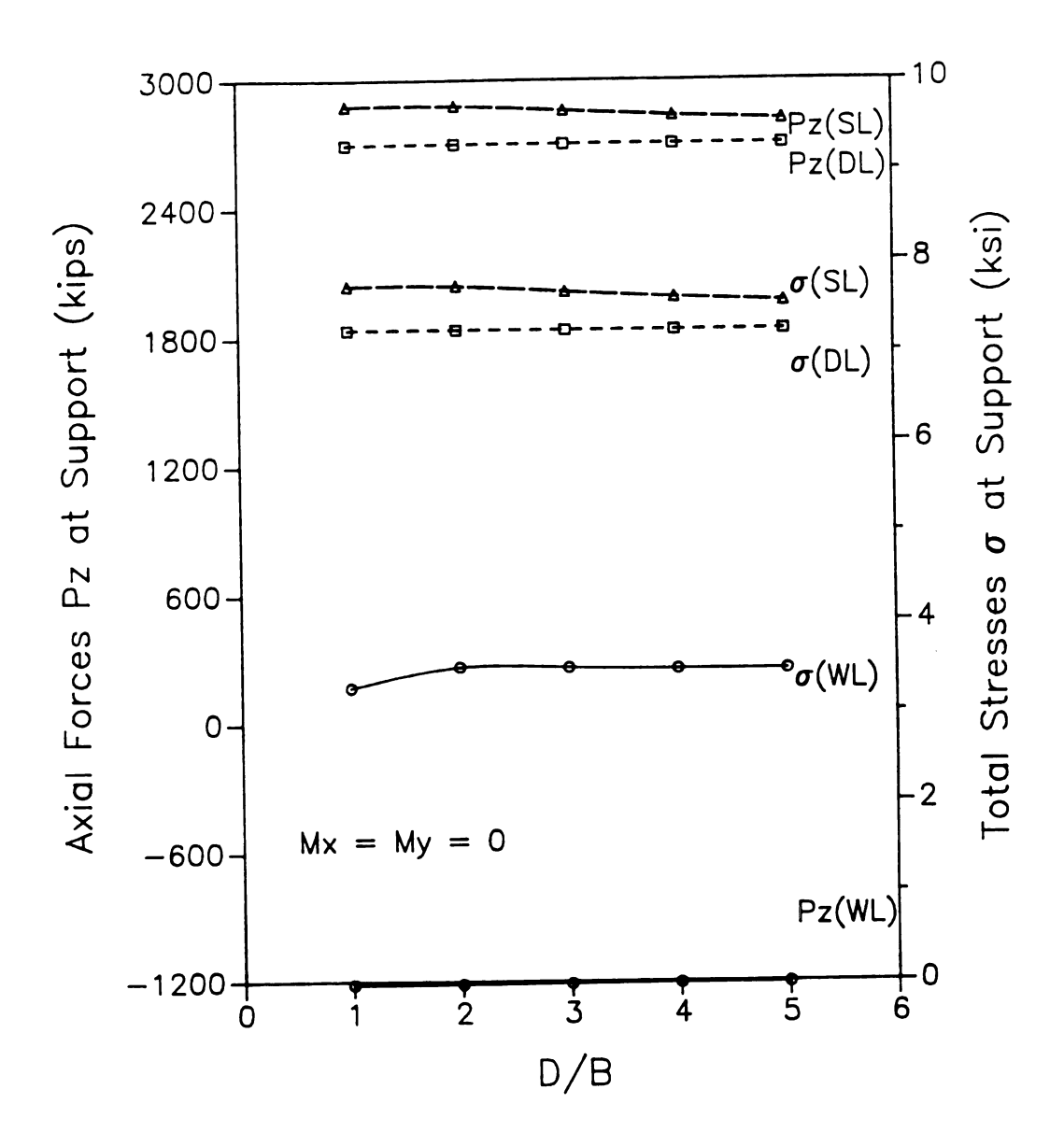


Figure 3-10. Stress and member forces at support due to varying D/B ratio (MCSCB).

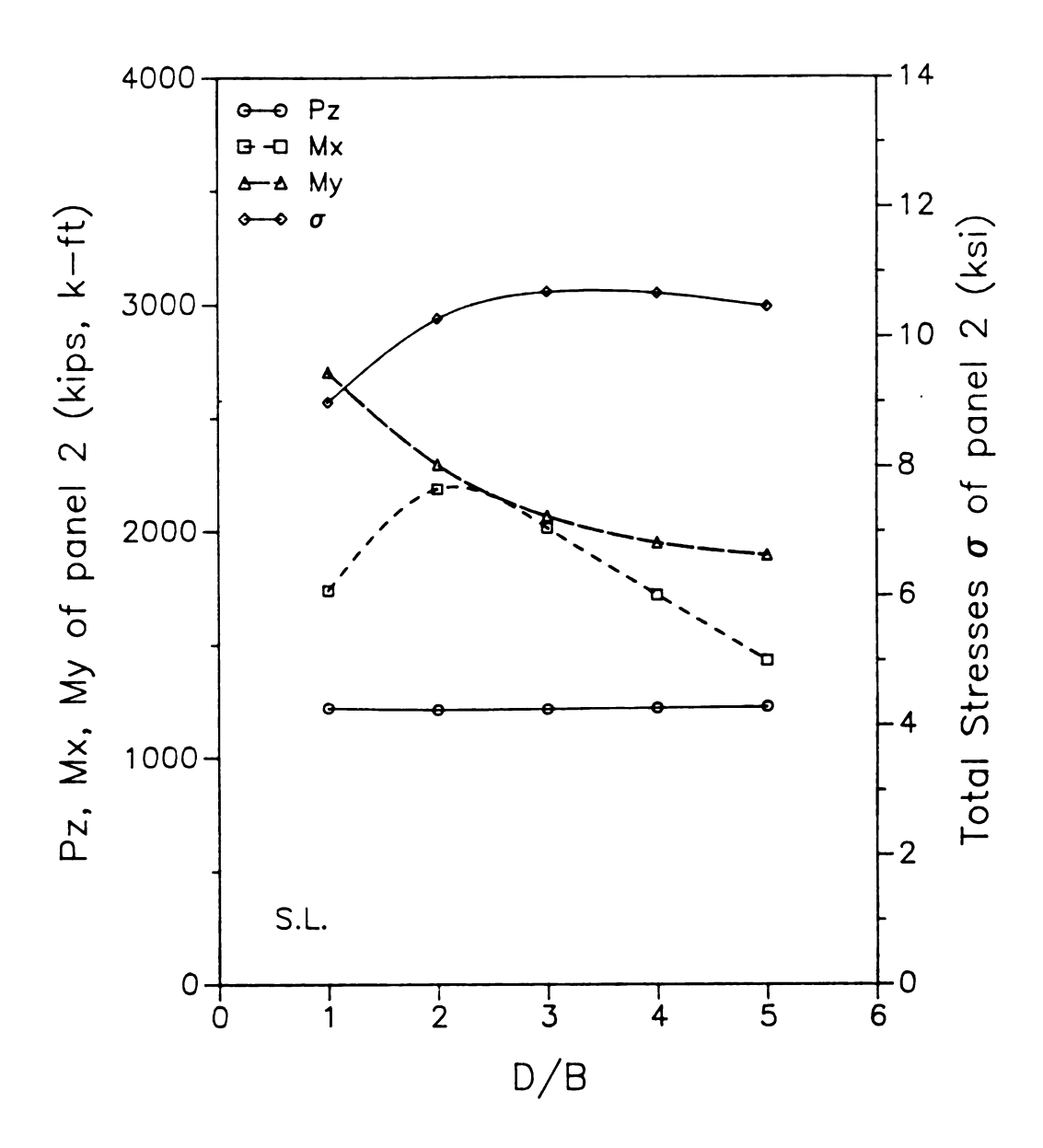


Figure 3-11. Stress and member forces at the left node of panel 2 due to varying D/B ratio (MCSCB), Z-motion seismic loading.

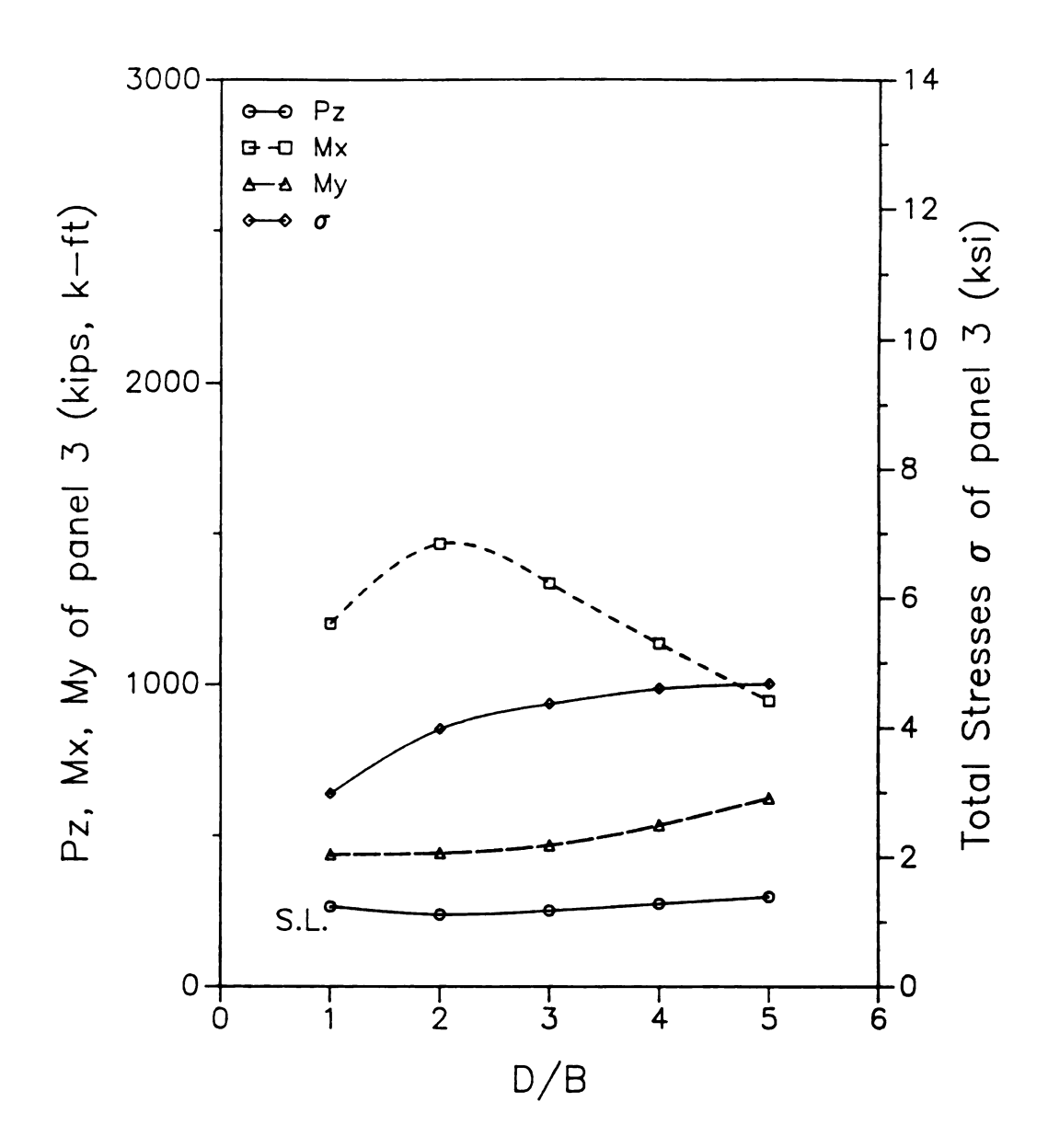


Figure 3-12. Stress and member forces at the left node of panel 3 due to varying D/B ratio (MCSCB), Z-motion seismic loading.

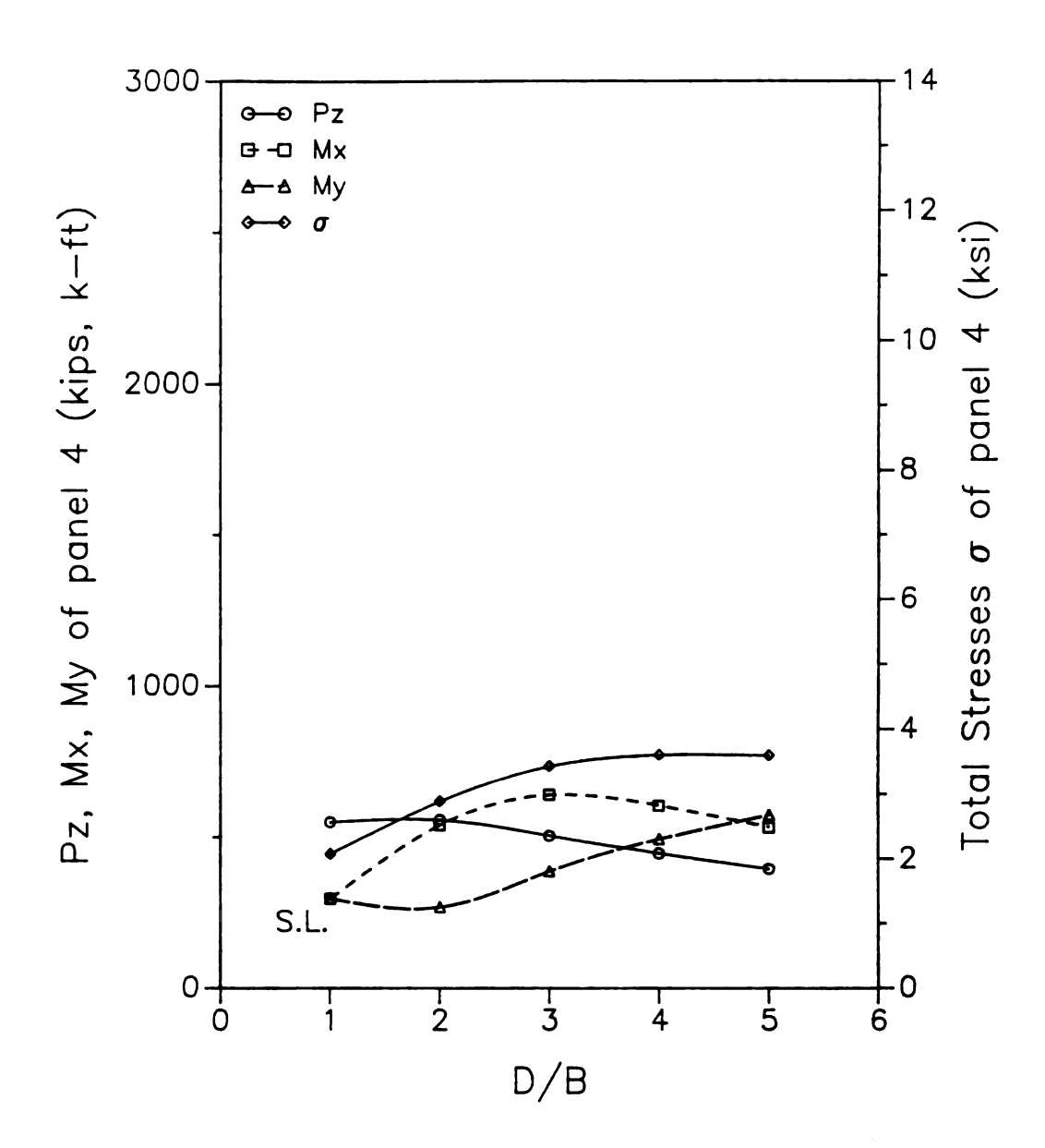


Figure 3-13. Stress and member forces at the left node of panel 4 due to varying D/B ratio (MCSCB), Z-motion seismic loading.

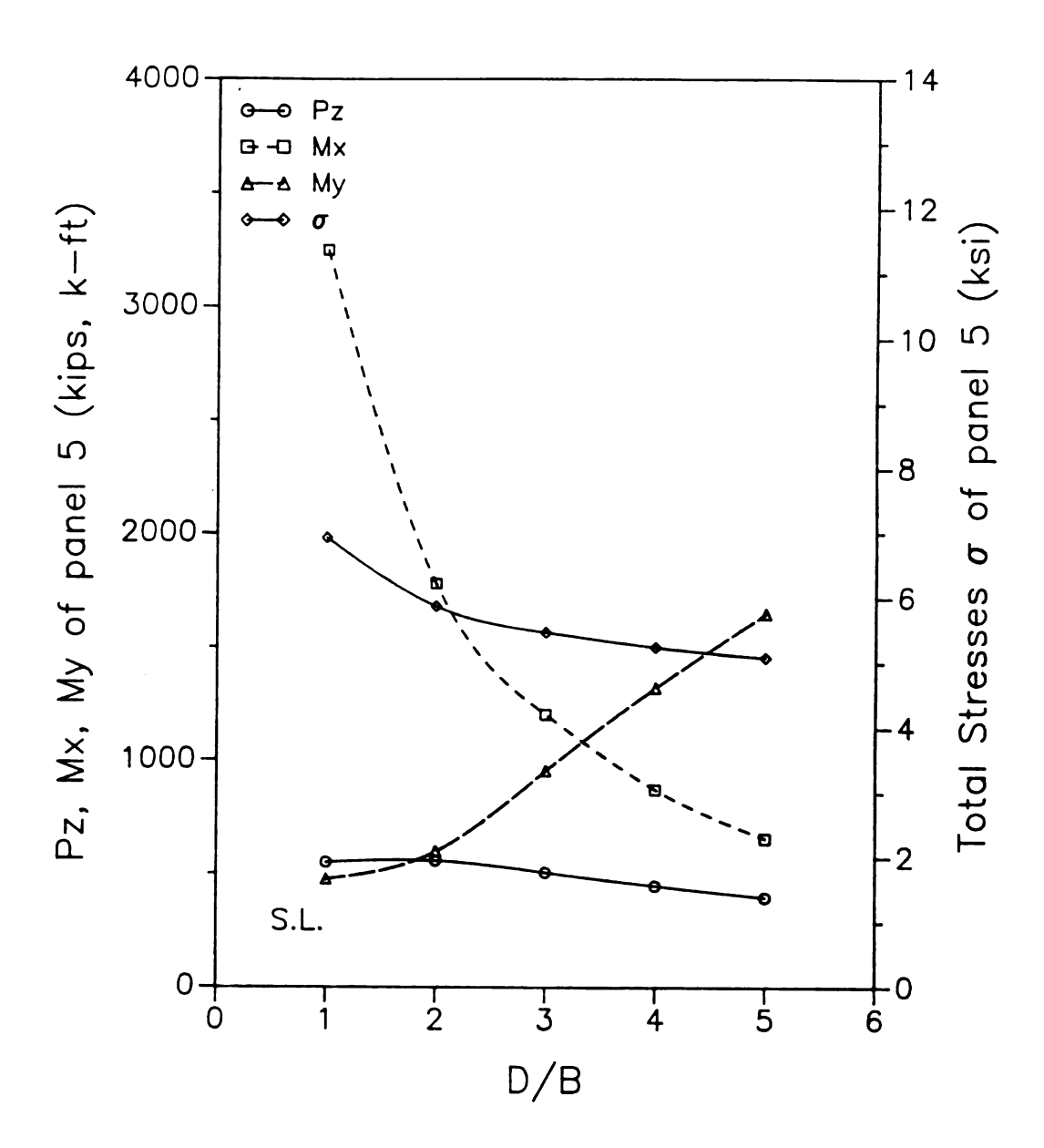


Figure 3-14. Stress and member forces at the left node of panel 5 due to varying D/B ratio (MCSCB), Z-motion seismic loading.

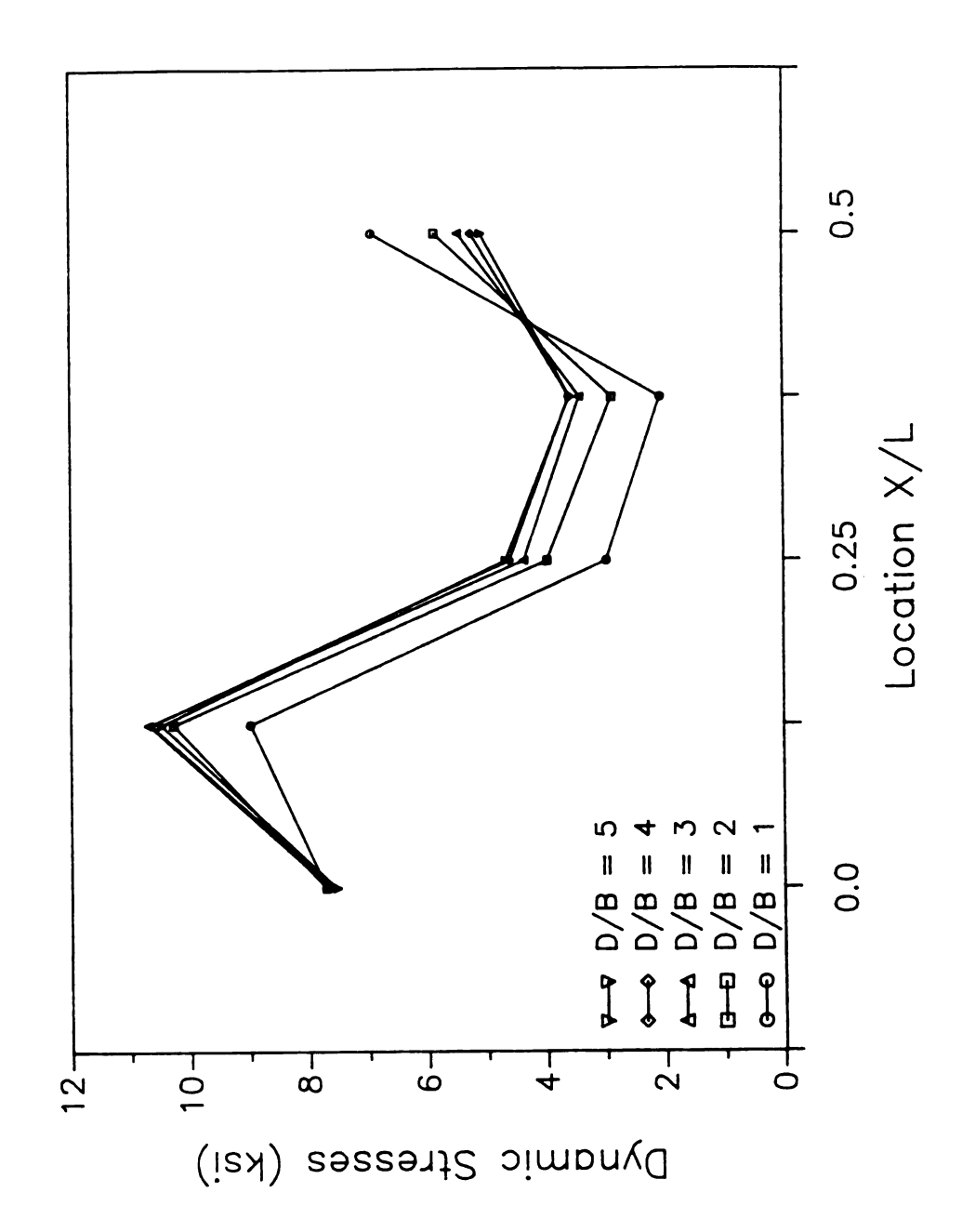


Figure 3-15. Dynamic stress distributions under lateral seismic loading (Z-motion) due to varying D/B ratio (MCSCB).

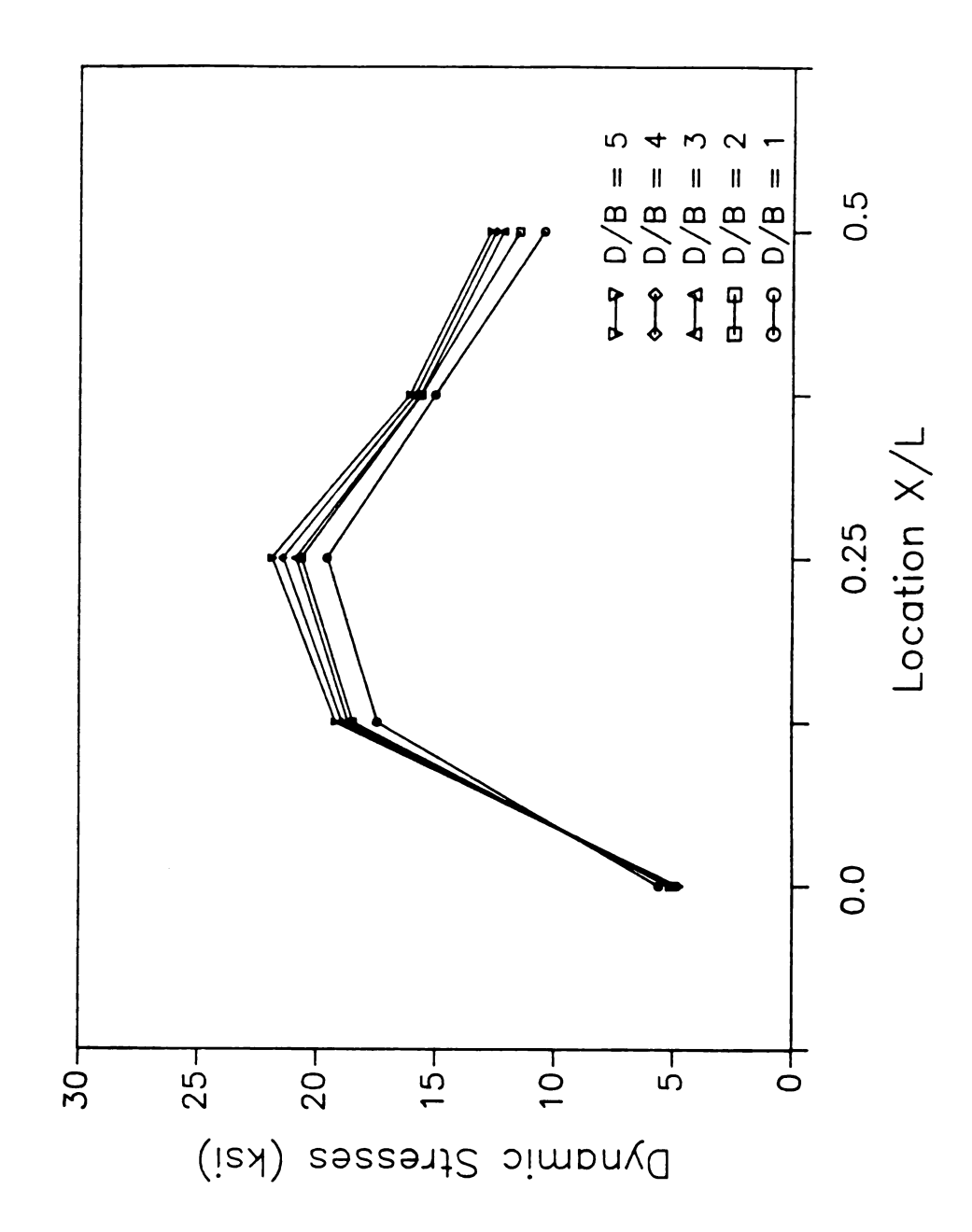


Figure 3-16. Dynamic stress distributions under in-plane seismic loading (X-, Y-motion) due to varying D/B ratio (MCSCB).

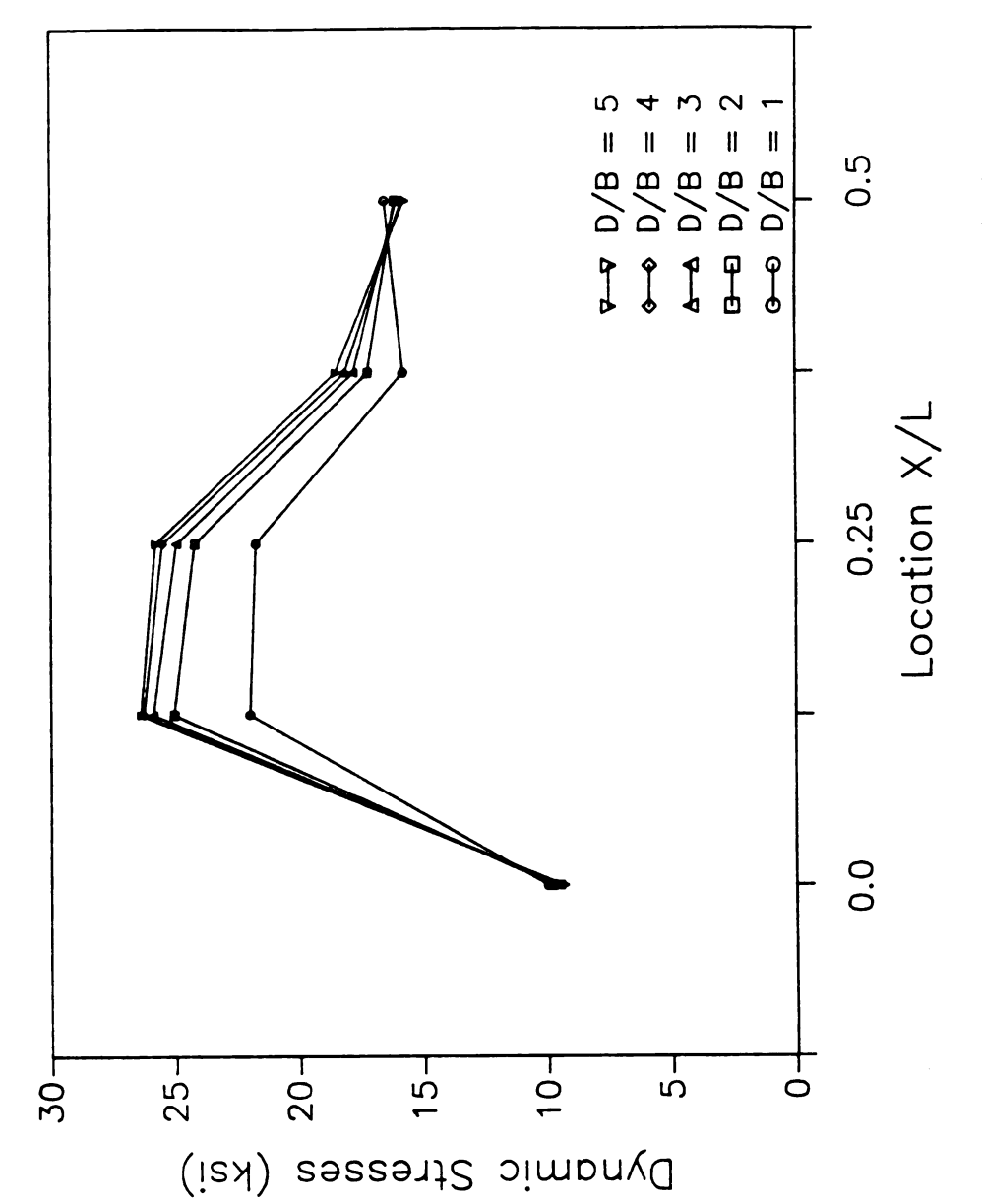


Figure 3-17. Dynamic stress distributions under three dimensional seismic

loading (X-, Y-, Z-motion) due to varying D/B ratio (MCSCB).

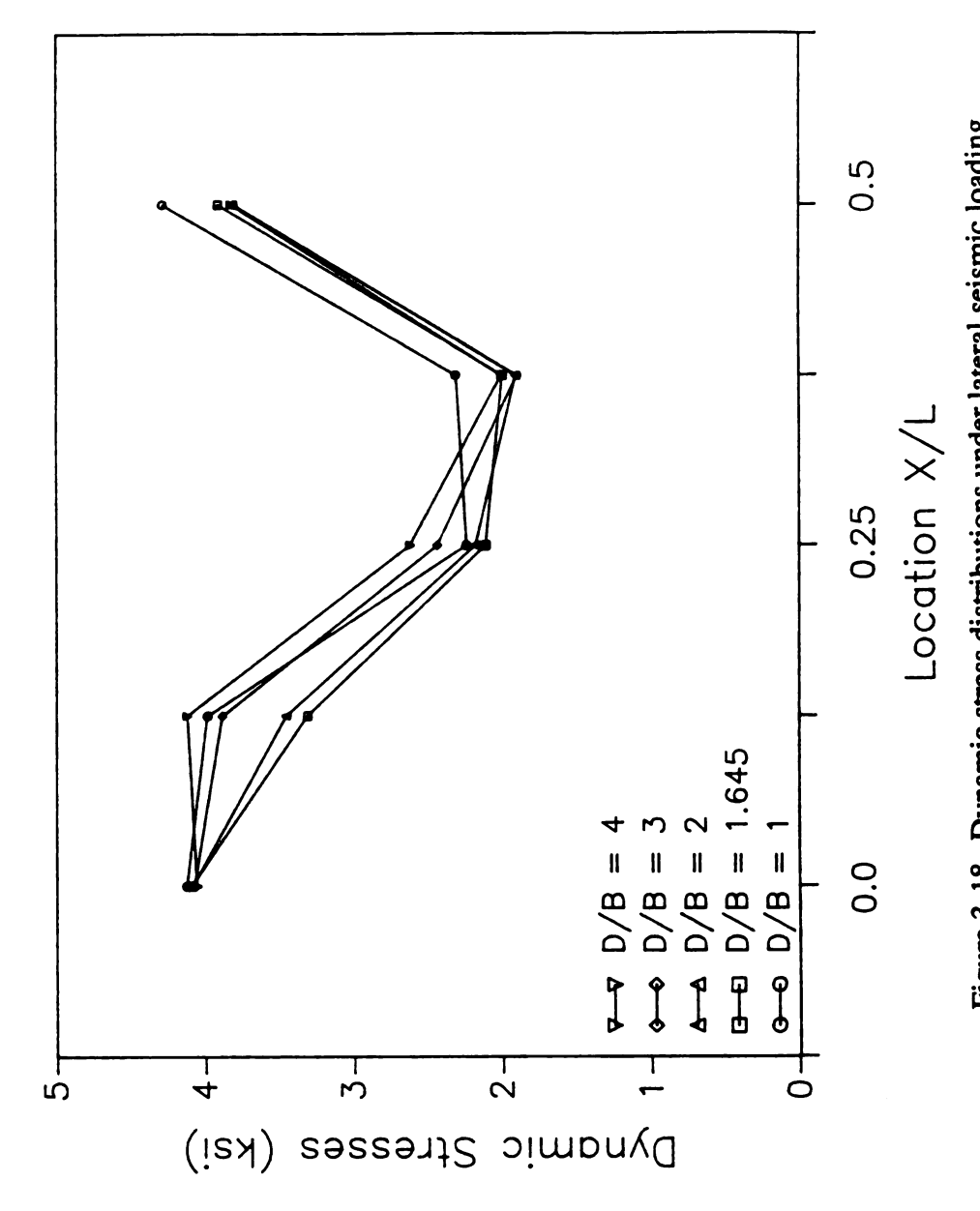


Figure 3-18. Dynamic stress distributions under lateral seismic loading

(Z-motion) due to varying D/B ratio (MSSB).

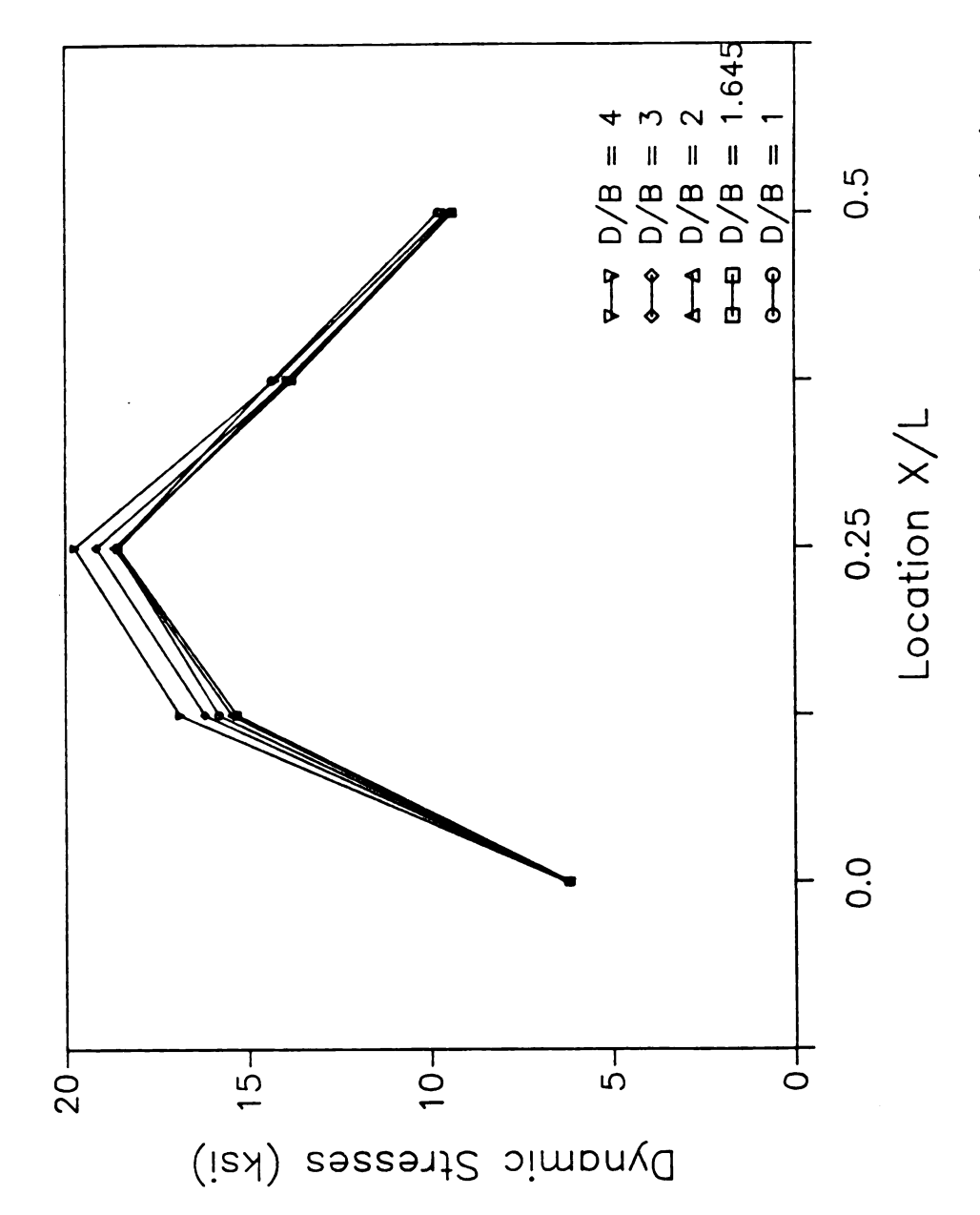


Figure 3-19. Dynamic stress distributions under three dimensional seismic loading (X-, Y-, Z-motion) due to varying D/B ratio (MSSB).

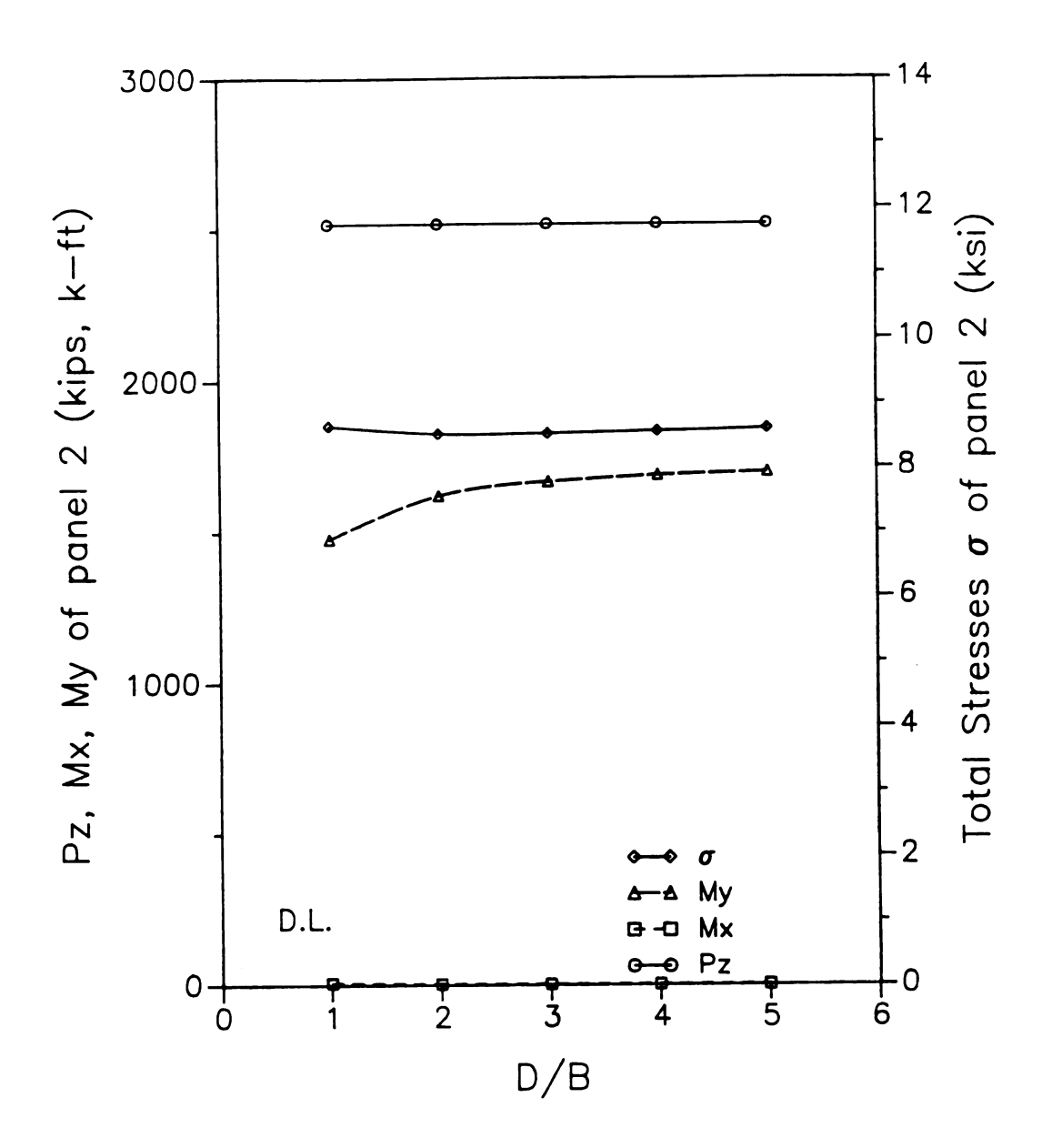


Figure 3 -20. Stress and member forces at the left node of panel 2 due to varying D/B ratio (MCSCB), dead load.

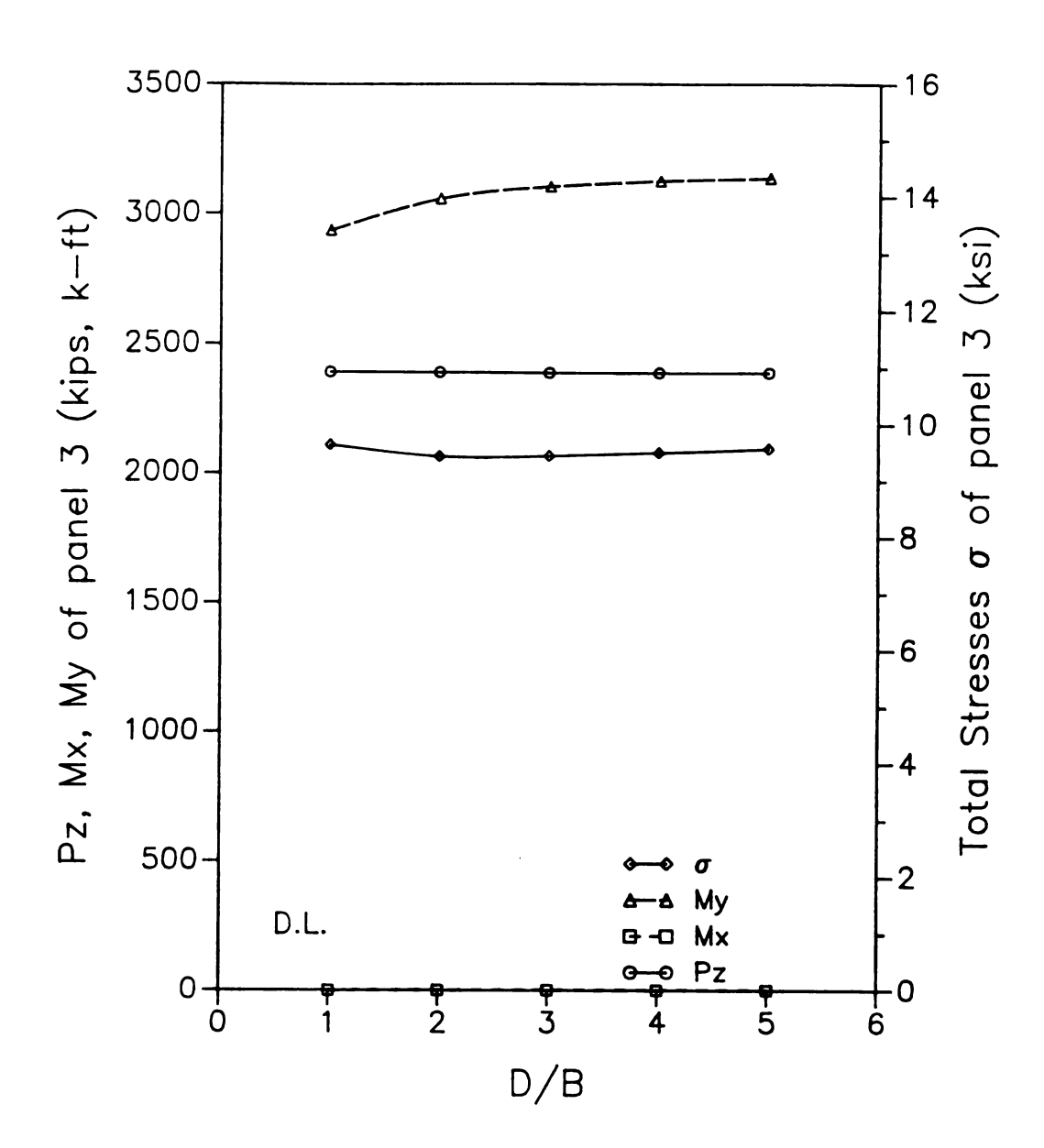


Figure 3 - 21. Stress and member forces at the left node of panel 3 due to varying D/B ratio (MCSCB), dead load.

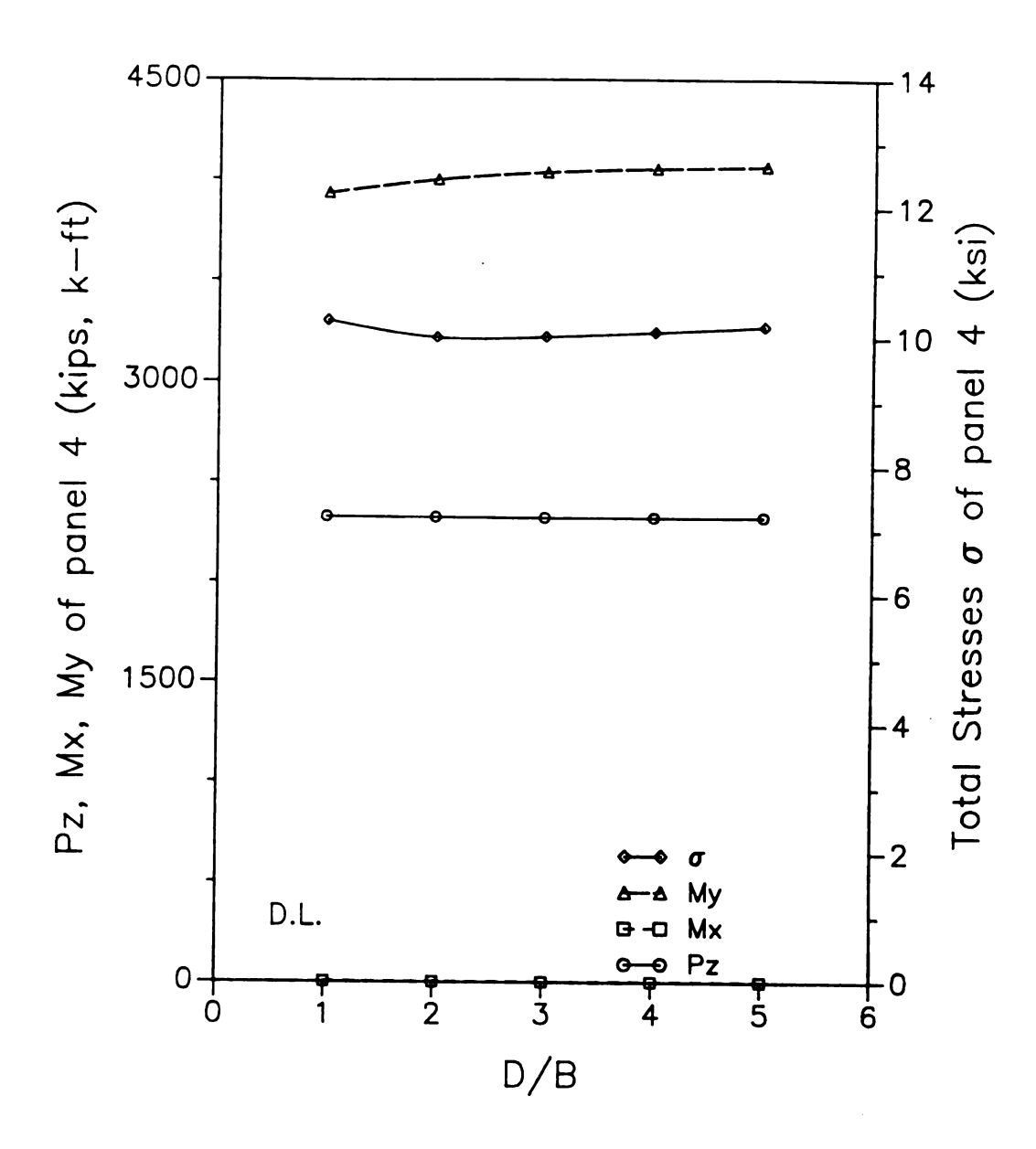


Figure 3 - 22. Stress and member forces at the left node of panel 4 due to varying D/B ratio (MCSCB), dead load.

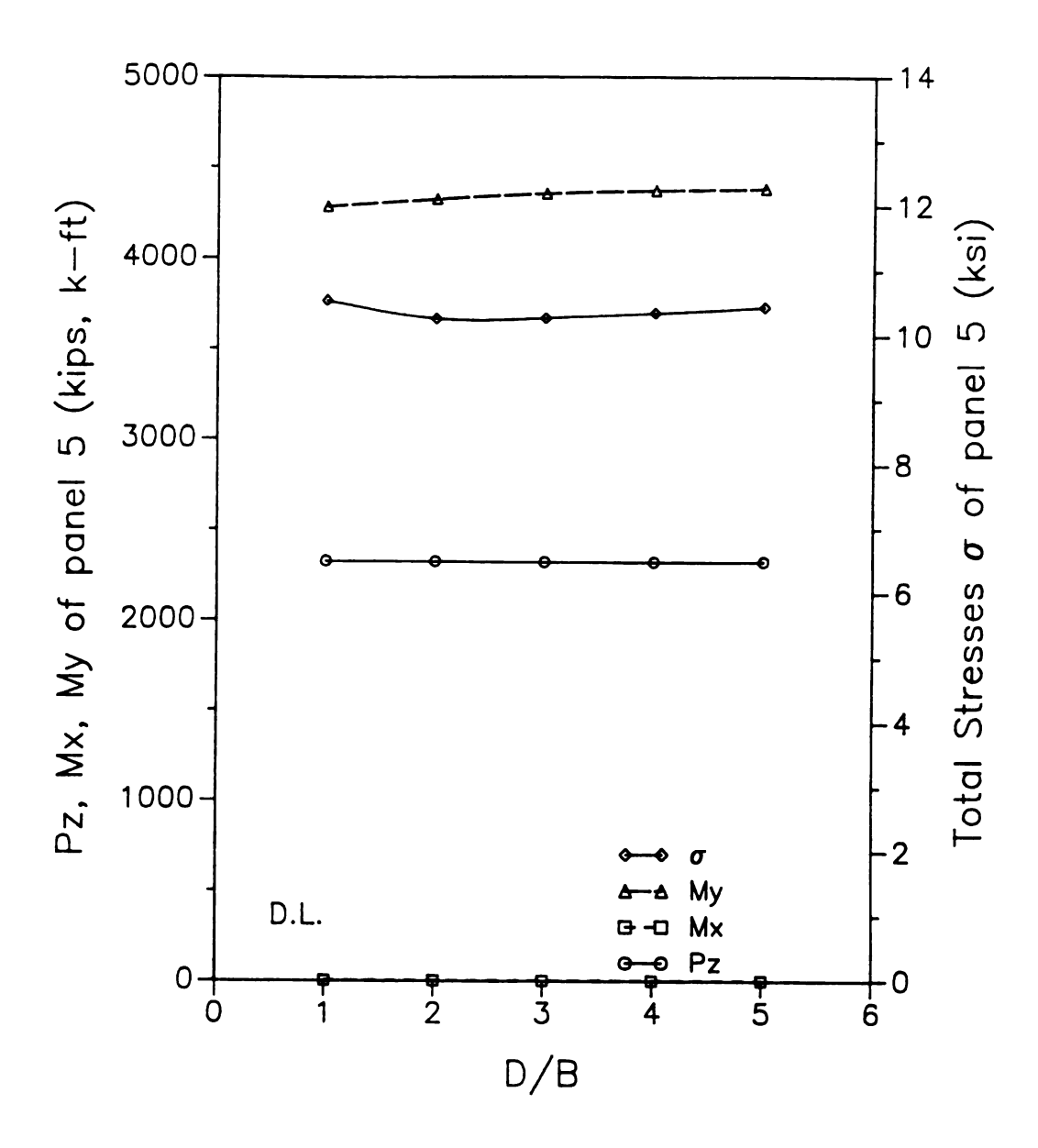


Figure 3 - 23. Stress and member forces at the left node of panel 5 due to varying D/B ratio (MCSCB), dead load.

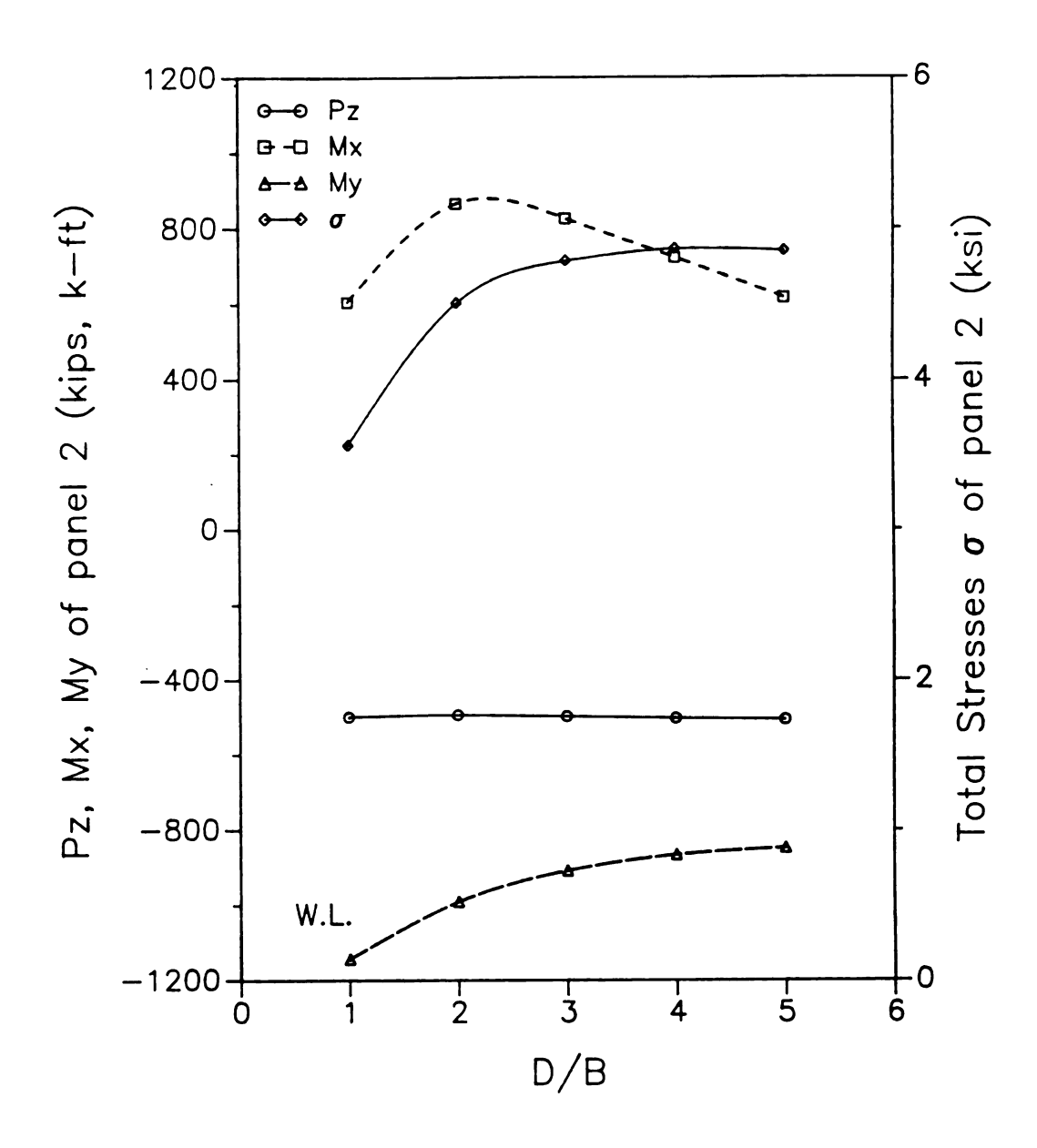


Figure 3 - 24. Stress and member forces at the left node of panel 2 due to varying D/B ratio (MCSCB), wind load.

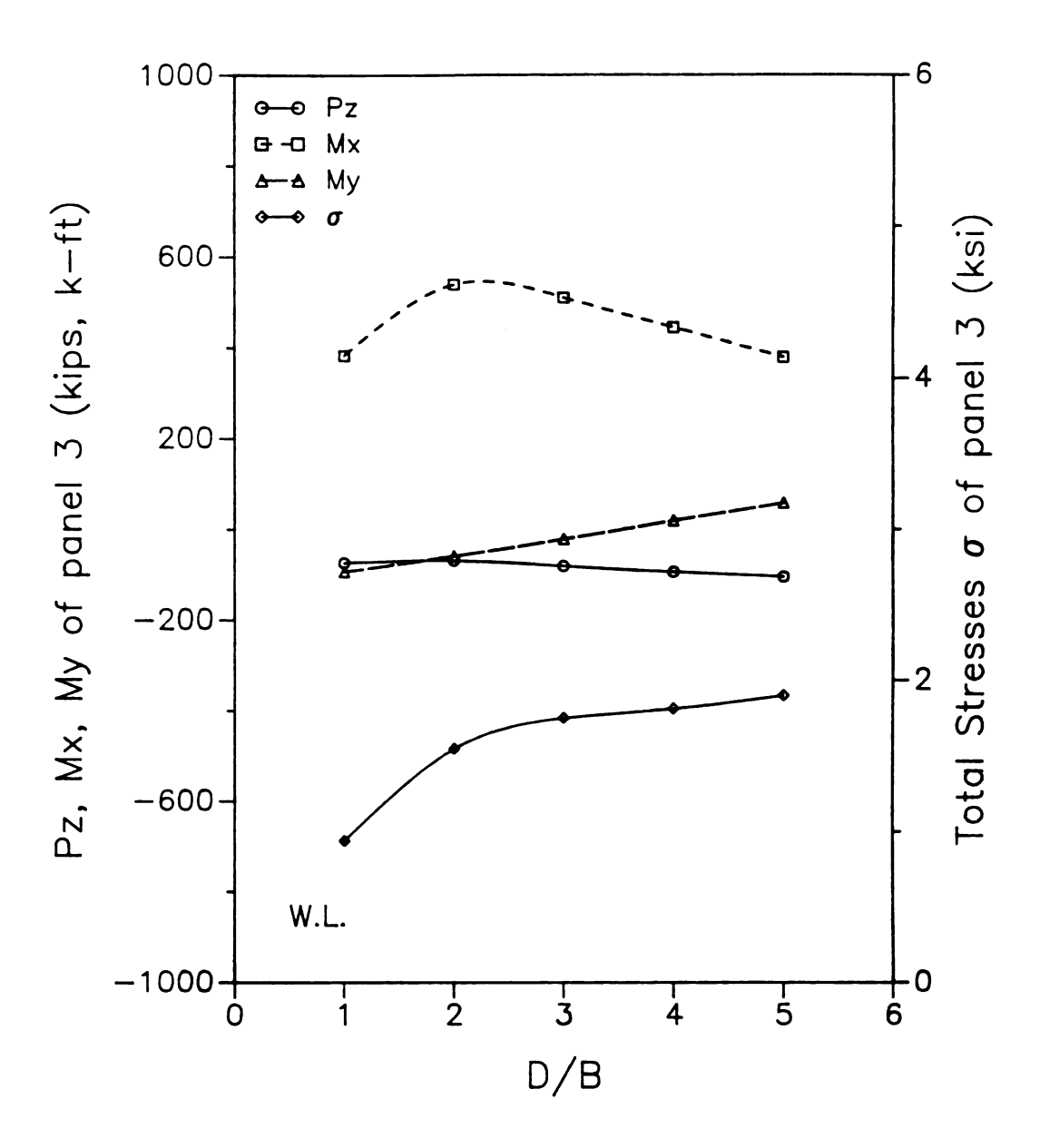


Figure 3 - 25. Stress and member forces at the left node of panel 3 due to varying D/B ratio (MCSCB), wind load.

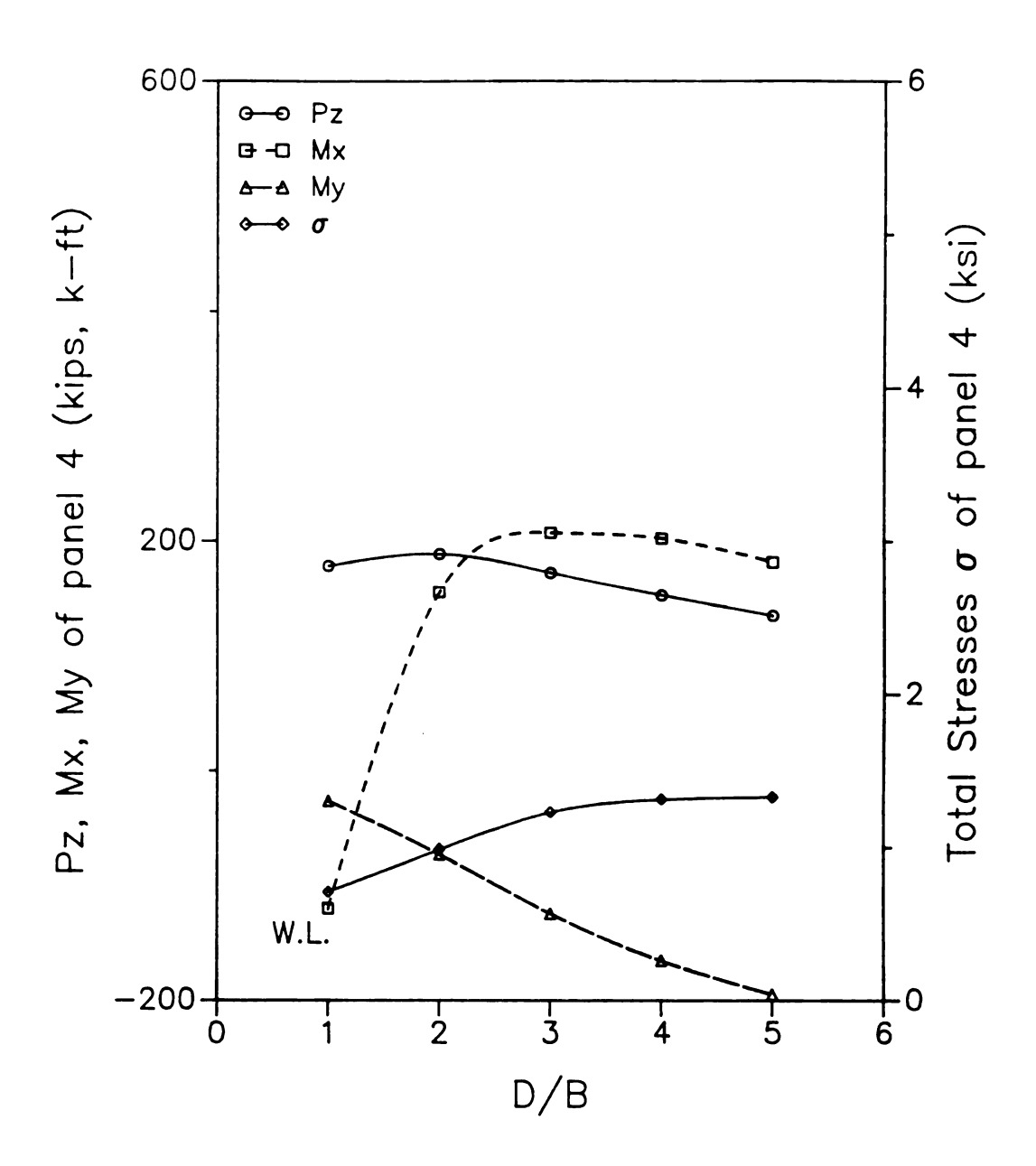


Figure 3 - 26. Stress and member forces at the left node of panel 4 due to varying D/B ratio (MCSCB), wind load.

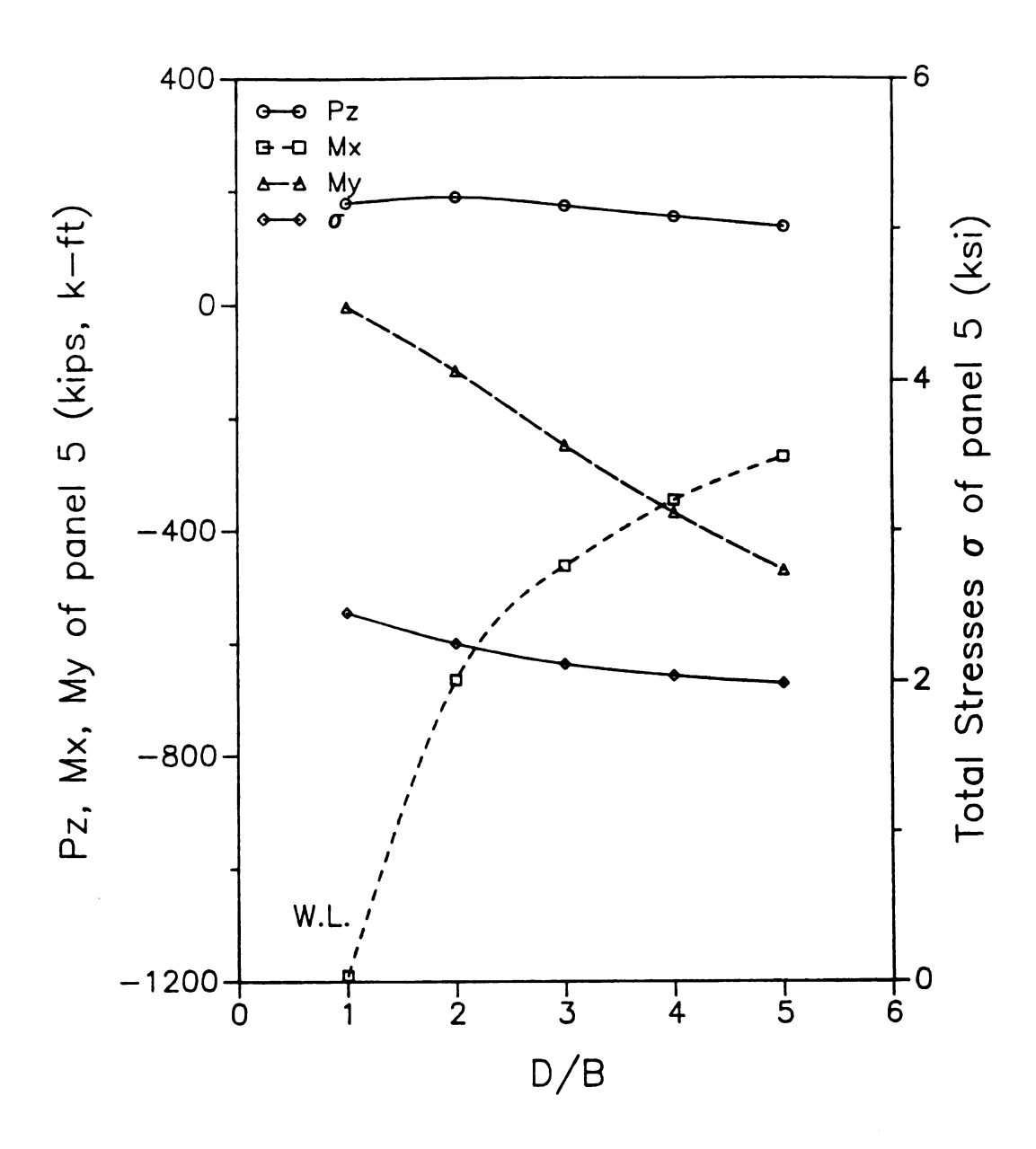


Figure 3 - 27. Stress and member forces at the left node of panel 5 due to varying D/B ratio (MCSCB), wind load.

CHAPTER IV SUMMARY AND CONCLUSION

4.1 Summary

The main purpose of this study is to provide information that could aid the designers of arch bridges in their decision regarding the two parameters: 1. column diagonal bracing and 2. the depth to width ratio of the rib box section. The designer basis is presumed to be elastic. Hence the chief measure of response is the maximum stress in the rib which is a combination of the effects of the axial force and the in-plane and out-of-bending moments. The study was based on a computer modelling of the bridge and load system. For the bridge, nonlinear elastic curved beam elements were used for the ribs (see Fig. 1-2), and straight beam elements were used for the cross-bracings between the ribs and the stringers of the deck. Truss elements were used for the cross-bracings between the ribs, for the column between the deck and the ribs, and for the deck system. The seismic load was represented by the design response spectrum of AASHTO. For better perspectives, dead load and wind load were also considered.

The dead load analysis was based on a nonlinear elastic analysis, the main feature of which was the consideration of the effect of the compression due to dead load on the stiffness of the ribs. That stiffness at the end of the dead load application was used as the linear stiffness for a linear dynamic analysis of the structure by use of the response spectrum and method of superposition. The CQC method of modal responses combination was adopted employing twenty normal modes.

Because of the large number of parameters involved, two real bridges were used for the study: the Cold Spring Canyon Bridge (CSCB) in California which has a span

length of 700 ft. and is relatively slender, and the South Street Bridge (SSB) in Connecticut which has a span of 193 ft. and is relatively stiff laterally. For the bridge models, a number of simplifications were made such as the number of panels and the exact geometry of the rib as well as the representation of the deck system. Hence they were referred to as modified versions or MCSCB and MSSB. The bulk of the data obtained pertains to MCSCB.

Before collecting the data for the major parameters for the study, a preliminary parametric study was made. It resulted in the decision to release the rotational constraints at the supports of the ribs, the choice of the deck stringer cross-sectional area and a multiplier for the torsional constant of the ribs.

For the column diagonal bracing, the cross-sectional area A_d was varied from 0.38 percent to 9 percent of that of the rib, and for the lower limit, bracing at the quarter point only was also considered. It was found that such lateral bracing was effective in reducing the maximum stress and the most effective schemes seems to use the smallest area, i.e., 0.38 percent, but use them at all panels.

The design parameter of the rib section depth to width D/B was varied from 1.0 to 5.0 with a fixed area of the rib cross-section and depth and web thickness ratio. For the MCSCB, it seems that the ratio of 1.0 is most effective. For the MSSB, the ratio of 1.65 seems to give the best results. Contrary to a general tendency in practice that such ratio would increase with longer spans, the results seem to indicate that the ratio need not go beyond two. The reason seems to lie in the fact that larger values of D/B do not increase the value of the section modulus for in-plane bending. That is, it does not strengthen the structure in the vertical direction while weakens it in the lateral direction.

For the same reason, an variation of D/B did not have a significant effect on the maximum stress due to dead load. Its effect on the wind load response is larger. The response to statically applied wind load is noted to be quite similar to the dynamic response to a lateral seismic load (horizontal motion normal to the bridge longitudinal axis). For the magnitude of the loading considered herein, the ratio between the stresses for the lateral seismic load and the wind load falls within the range of 2.4 to 2.9. This is

also true for member forces. Thus for consideration of the lateral seismic loading, a reasonably good estimation may be obtained from a static wind load analysis.

4.2 Concluding Remarks

The design parameters: the size of the cross-sectional area of the column diagonal bracing, and the depth to width ratio of the rib section, are studied for an effective seismic design of the deck type of arch bridges. Responses to dead load and wind load are also considered. The results provide considerable insight into the behavior of such bridges and guidance to their seismic design.

Because of the large number of parameters involved in the system, it is infeasible to produce general formulas or even tables or charts as design aids. However, the information presented here should be useful in providing guidance for an initial design. A final design still need be done with the aid of a computer program using a more precise modelling of the structure proposed. For an elastic design, it is appropriate to use the tangent stiffness of ribs as the stiffness for a linear dynamic analysis.

LIST OF REFERENCES

LIST OF REFERENCES

- 1. Bellamine, A. 1992. Seismic response of tied arch bridges. M.S. Thesis, Department of Civil Engineering, Michigan State University, E. Lansing, MI, 1992.
- 2. Clough, R. W. and J. Penzien, Dynamics of Structure. McGraw-Hill Book Company, New York, 1975.
- 3. Dusseau, R. A. and R. K. Wen, "Seismic Responses of Deck-Type Arch Bridges", Earthquake Engineering and Structural Dynamics, Vol.18, pp.701-715, 1989.
- 4. Garbow, B.S. "Subroutine RSG". Mathematics and Computer Science Div., Argonne National Laboratory, 1983.
- 5. Lange, J., "Elastic Buckling of Arches by Finite Element Method", Ph.D. Dissertation, Department of Civil Engineering, Michigan State University, E. Lansing, MI, 1980.
- 6. Lee, C. M., "Nonlinear Seismic Analysis of Steel Arch Bridges", Ph.D. Dissertation, Department of Civil Engineering, Michigan State University, E. Lansing, MI. 1990.
- 7. Lee, H. E. and M. A. M. Torkamani, 1989. Dynamic response of tied arch bridges to earthquake excitations, Department of Civil Engineering, University of Pittsburgh. Pittsburgh, Pennsylvania.
- 8. Merrit, F. S. Editor, Structural steel designers' handbook. Section 13, McGraw-Hill Book Company, New York, 1972.
- 9. Millies, R. J., "Three Dimensional Elastic Seismic Response of Deck Type Arch Bridges", M.S.Thesis, Department of Civil Engineering, Michigan State University, E.Lansing, MI 1992.
- 10. Raithel, A., and Franciosi.C., "Dynamic Response of Arches Using Lagrangian Approach", Journal of Structural Engineering, April 1984, pp. 847-858.

LIST OF REFERENCES(continued)

- 11. Standard Specifications For Seismic Design of Highway Bridges, 1983. American Association of State Highway and Transportation Officials. Washington, D.C.
- 12. U.S. Department of Transportation, "Arch Bridges", Series No.2, Washington D.C., 1977.
- 13. Wen, R. K., and B. Suhendro "Nonlinear Curved-Beam Element for Arch Structures", Journal of Structural Engineering, ASCE, Vol. 117, No.11, Nov. 1991, pp. 3496-3515.
- Wen, R. K., "Seismic Behavior and Design of Arch Bridges", Proceedings of the 4th U.S. National Conference On Earthquake Engineering, Palm Springs, California, May 1990, Vol.1, pp. 1027-1036.
- 15. Wen, R. K., C. M. Lee and Alahamd, "Incremental Resistance and Deformations of Elasto-plastic Beams, Journal of Structural Engineering, ASCE, Vol. 115, No.5, Nov. 1989, pp. 1267-1271.

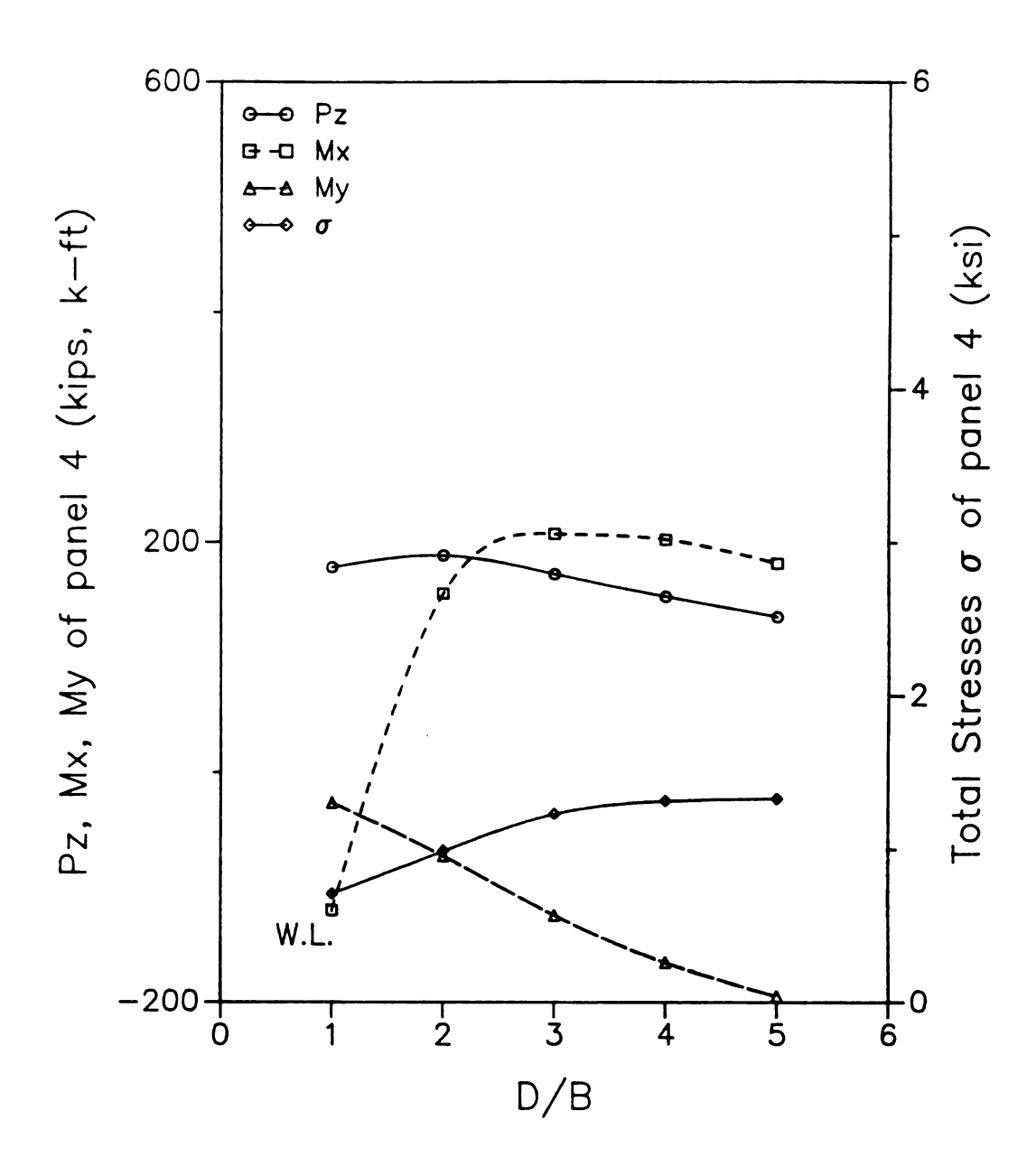


Figure 3 - 26. Stress and member forces at the left node of panel 4 due to varying D/B ratio (MCSCB), wind load.

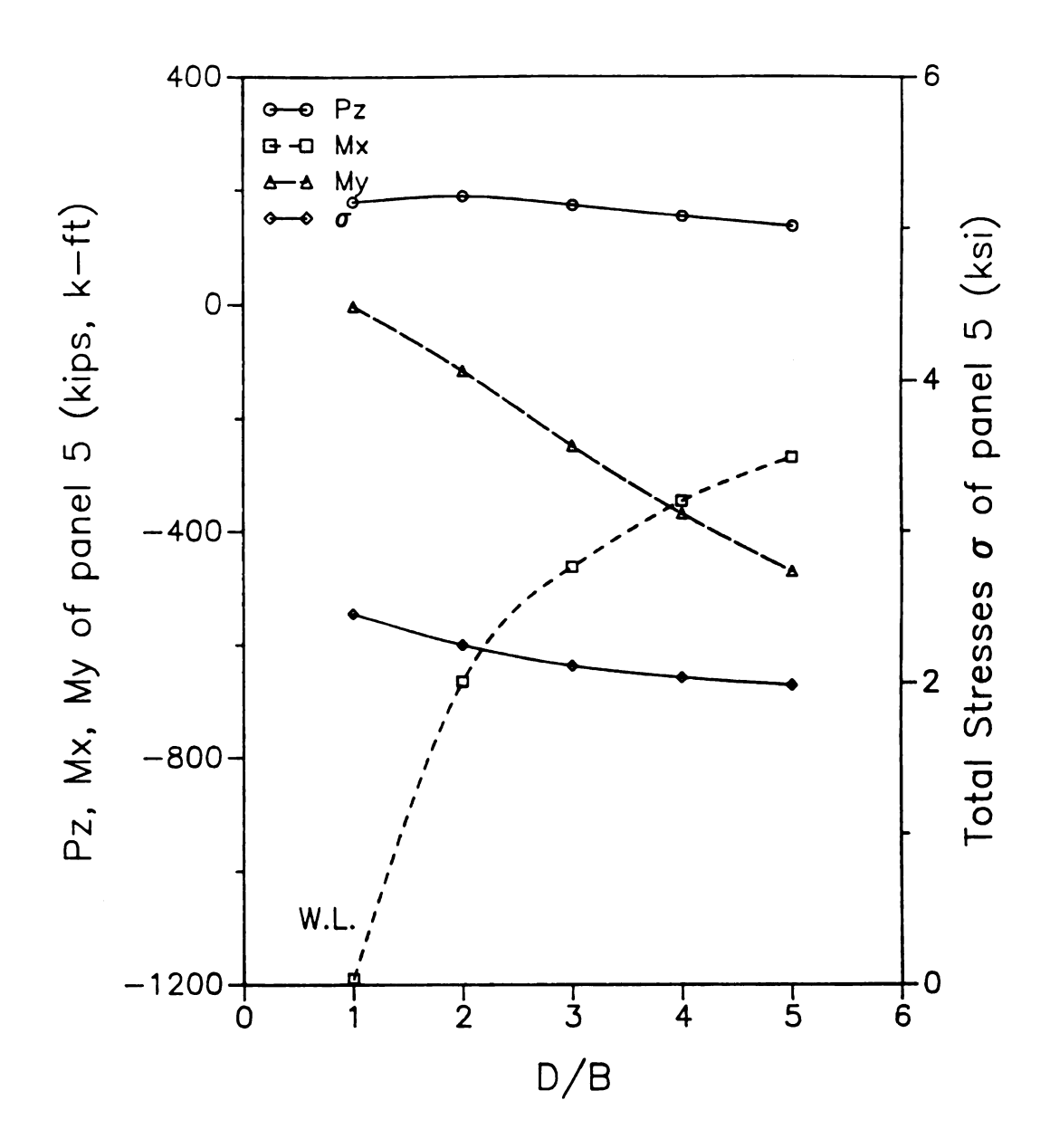


Figure 3 - 27. Stress and member forces at the left node of panel 5 due to varying D/B ratio (MCSCB), wind load.

CHAPTER IV SUMMARY AND CONCLUSION

4.1 Summary

The main purpose of this study is to provide information that could aid the designers of arch bridges in their decision regarding the two parameters: 1. column diagonal bracing and 2. the depth to width ratio of the rib box section. The designer basis is presumed to be elastic. Hence the chief measure of response is the maximum stress in the rib which is a combination of the effects of the axial force and the in-plane and out-of-bending moments. The study was based on a computer modelling of the bridge and load system. For the bridge, nonlinear elastic curved beam elements were used for the ribs (see Fig. 1-2), and straight beam elements were used for the cross bars between the ribs and the stringers of the deck. Truss elements were used for the cross-bracings between the ribs, for the column between the deck and the ribs, and for the deck system. The seismic load was represented by the design response spectrum of AASHTO. For better perspectives, dead load and wind load were also considered.

The dead load analysis was based on a nonlinear elastic analysis, the main feature of which was the consideration of the effect of the compression due to dead load on the stiffness of the ribs. That stiffness at the end of the dead load application was used as the linear stiffness for a linear dynamic analysis of the structure by use of the response spectrum and method of superposition. The CQC method of modal responses combination was adopted employing twenty normal modes.

Because of the large number of parameters involved, two real bridges were used for the study: the Cold Spring Canyon Bridge (CSCB) in California which has a span

length of 700 ft. and is relatively slender, and the South Street Bridge (SSB) in Connecticut which has a span of 193 ft. and is relatively stiff laterally. For the bridge models, a number of simplifications were made such as the number of panels and the exact geometry of the rib as well as the representation of the deck system. Hence they were referred to as modified versions or MCSCB and MSSB. The bulk of the data obtained pertains to MCSCB.

Before collecting the data for the major parameters for the study, a preliminary parametric study was made. It resulted in the decision to release the rotational constraints at the supports of the ribs, the choice of the deck stringer cross-sectional area and a multiplier for the torsional constant of the ribs.

For the column diagonal bracing, the cross-sectional area A_d was varied from 0.38 percent to 9 percent of that of the rib, and for the lower limit, bracing at the quarter point only was also considered. It was found that such lateral bracing was effective in reducing the maximum stress and the most effective schemes seems to use the smallest area, i.e., 0.38 percent, but use them at all panels.

The design parameter of the rib section depth to width D/B was varied from 1.0 to 5.0 with a fixed area of the rib cross-section and depth and web thickness ratio. For the MCSCB, it seems that the ratio of 1.0 is most effective. For the MSSB, the ratio of 1.65 seems to give the best results. Contrary to a general tendency in practice that such ratio would increase with longer spans, the results seem to indicate that the ratio need not go beyond two. The reason seems to lie in the fact that larger values of D/B do not increase the value of the section modulus for in-plane bending. That is, it does not strengthen the structure in the vertical direction while weakens it in the lateral direction.

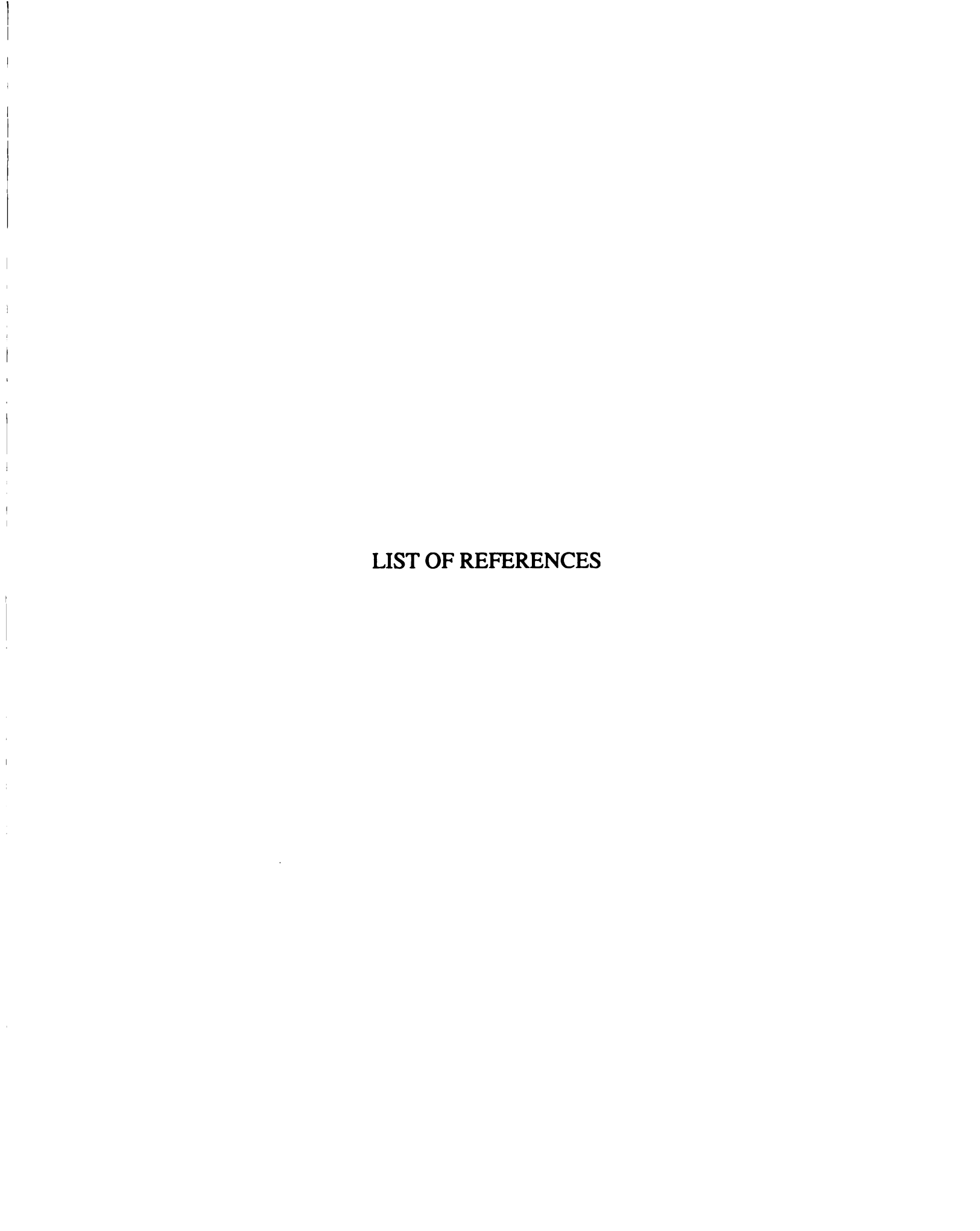
For the same reason, an variation of D/B did not have a significant effect on the maximum stress due to dead load. Its effect on the wind load response is larger. The response to statically applied wind load is noted to be quite similar to the dynamic response to a lateral seismic load (horizontal motion normal to the bridge longitudinal axis). For the magnitude of the loading considered herein, the ratio between the stresses for the lateral seismic load and the wind load falls within the range of 2.4 to 2.9. This is

also true for member forces. Thus for consideration of the lateral seismic loading, a reasonably good estimation may be obtained from a static wind load analysis.

4.2 Concluding Remarks

The design parameters: the size of the cross-sectional area of the column diagonal bracing, and the depth to width ratio of the rib section, are studied for an effective seismic design of the deck type of arch bridges. Responses to dead load and wind load are also considered. The results provide considerable insight into the behavior of such bridges and guidance to their seismic design.

Because of the large number of parameters involved in the system, it is infeasible to produce general formulas or even tables or charts as design aids. However, the information presented here should be useful in providing guidance for an initial design. A final design still need be done with the aid of a computer program using a more precise modelling of the structure proposed. For an elastic design, it is appropriate to use the tangent stiffness of ribs as the stiffness for a linear dynamic analysis.



LIST OF REFERENCES

- 1. Bellamine, A. 1992. Seismic response of tied arch bridges. M.S. Thesis, Department of Civil Engineering, Michigan State University, E. Lansing, MI, 1992.
- 2. Clough, R. W. and J. Penzien, Dynamics of Structure. McGraw-Hill Book Company, New York, 1975.
- 3. Dusseau, R. A. and R. K. Wen, "Seismic Responses of Deck-Type Arch Bridges", Earthquake Engineering and Structural Dynamics, Vol.18, pp.701-715, 1989.
- 4. Garbow, B.S. "Subroutine RSG". Mathematics and Computer Science Div., Argonne National Laboratory, 1983.
- 5. Lange, J., "Elastic Buckling of Arches by Finite Element Method", Ph.D. Dissertation, Department of Civil Engineering, Michigan State University, E. Lansing, MI, 1980.
- 6. Lee, C. M., "Nonlinear Seismic Analysis of Steel Arch Bridges", Ph.D. Dissertation, Department of Civil Engineering, Michigan State University, E. Lansing, MI. 1990.
- 7. Lee, H. E. and M. A. M. Torkamani, 1989. Dynamic response of tied arch bridges to earthquake excitations, Department of Civil Engineering, University of Pittsburgh. Pittsburgh, Pennsylvania.
- 8. Merrit, F. S. Editor, Structural steel designers' handbook. Section 13, McGraw-Hill Book Company, New York, 1972.
- 9. Millies, R. J., "Three Dimensional Elastic Seismic Response of Deck Type Arch Bridges", M.S.Thesis, Department of Civil Engineering, Michigan State University, E.Lansing, MI 1992.
- 10. Raithel, A., and Franciosi.C., "Dynamic Response of Arches Using Lagrangian Approach", Journal of Structural Engineering, April 1984, pp. 847-858.

LIST OF REFERENCES(continued)

- 11. Standard Specifications For Seismic Design of Highway Bridges, 1983. American Association of State Highway and Transportation Officials. Washington, D.C.
- 12. U.S. Department of Transportation, "Arch Bridges", Series No.2, Washington D.C., 1977.
- 13. Wen, R. K., and B. Suhendro "Nonlinear Curved-Beam Element for Arch Structures", Journal of Structural Engineering, ASCE, Vol. 117, No.11, Nov. 1991, pp. 3496-3515.
- 14. Wen, R. K., "Seismic Behavior and Design of Arch Bridges", Proceedings of the 4th U.S. National Conference On Earthquake Engineering, Palm Springs, California, May 1990, Vol.1, pp. 1027-1036.
- 15. Wen, R. K., C. M. Lee and Alahamd, "Incremental Resistance and Deformations of Elasto-plastic Beams, Journal of Structural Engineering, ASCE, Vol. 115, No.5, Nov. 1989, pp. 1267-1271.

